

***IN VIVO* INVESTIGATION OF TALIN, TENSIN AND INTEGRIN-LINKED  
KINASE DYNAMICS AT STABLE CELL-EXTRACELLULAR MATRIX  
ADHESIONS**

by

Stefan Czerniecki

B.Sc., McGill University, 2010

A THESIS SUBMITTED IN PARTIAL FULFILLMENT OF  
THE REQUIREMENTS FOR THE DEGREE OF

MASTER OF SCIENCE

in

THE FACULTY OF GRADUATE STUDIES

(Cell and Developmental Biology)

THE UNIVERSITY OF BRITISH COLUMBIA

(Vancouver)

April 2013

© Stefan Czerniecki, 2013

## Abstract

Cell-extra cellular matrix (ECM) adhesion through the integrin family of receptors is required for metazoan development, and throughout adult life. Elucidating the mechanisms that regulate this adhesion is fundamental to understanding how animals create and maintain tissue architecture. Modulating adhesion assembly and disassembly is one of the key ways in which adhesion strength and integrity is regulated. We concentrate on analyzing the dynamics of three important components of the integrin adhesion complex (IAC), talin, tensin, and ILK, to determine how they function as mechano-sensory components of cell-ECM adhesions in the context of a living, multicellular organism, *Drosophila melanogaster*. We utilize fluorescently-tagged proteins under conditions of altered mechanical force, combined with a specialized fluorescence recovery after photobleaching (FRAP) protocol, to examine the dynamics of talin, tensin, and ILK. We subsequently use advanced mathematical modeling to gain mechanistic insight into how protein turnover is modified by tensile force. Furthermore, we attempt to clarify the role of key talin domains in mechanosensation, using FRAP and *Drosophila* homologs of previously characterized talin mutations, under conditions of altered force. The results outlined in this work show that talin mobility is directly regulated by force in an intact, complex organism at sites of stable adhesion between integrins and the ECM. Moreover, the results indicate that the mobility change due to increased force is a robust process, and not easily disrupted by mutating talin domains. Changes in talin dynamics when force is reduced is an active process, and is dependent on both the physical linkage of talin to integrin, and the ability of talin to auto-inhibit. Furthermore, studies of talin, tensin, and ILK turnover with high-temporal resolution uncover

the intricacies of adhesion regulation in response to changing environmental conditions, with talin primarily regulated on the level of recycling, tensin regulated by a mix of both recycling and binding, and ILK regulated through control of binding.

## **Preface**

Guy Tanentzapf and Stefan Czerniecki designed work presented in this thesis. Stefan Czerniecki performed all the fly genetics, collected, analyzed, and interpreted all the FRAP data, and produced all the figures. Michael J. Fairchild produced the talin mutant constructs, and Raibatak Das designed the mathematical method to integrate and model the high-temporal resolution FRAP data, and calculated the rate constants associated with those experiments.

# Table of Contents

<b>Abstract.....</b>	<b>ii</b>
<b>Preface.....</b>	<b>iv</b>
<b>Table of Contents .....</b>	<b>v</b>
<b>List of Tables .....</b>	<b>viii</b>
<b>List of Figures.....</b>	<b>ix</b>
<b>Acknowledgements .....</b>	<b>xi</b>
<b>Dedication .....</b>	<b>xii</b>
<b>Chapter 1: Introduction .....</b>	<b>1</b>
1.1 Mechanotransduction.....	1
1.2 Cell adhesion.....	5
1.2.1 Integrins and the ECM.....	8
1.3 The integrin adhesion complex.....	9
1.3.1 Talin .....	11
1.3.2 Tensin.....	16
1.3.3 Integrin-linked kinase .....	17
1.4 Integrins as mechanosensors.....	19
1.4.1 Integrin directly responds to force .....	19
1.4.2 The integrin adhesion complex is also directly modulated by force .....	21
1.5 Integrin turnover .....	23
1.5.1 Fluorescence recovery after photobleaching .....	23
1.5.2 Integrin adhesion disassembly and recycling .....	26

1.5.3	Integrin adhesion complex disassembly .....	26
1.6	Objectives, rationale, hypothesis .....	27
<b>Chapter 2: Materials and Methods .....</b>		<b>32</b>
2.1	Fly stocks .....	32
2.2	FRAP experiments and statistical analysis .....	32
2.3	Mathematical modeling of IAC protein dynamics.....	33
<b>Chapter 3: Results.....</b>		<b>36</b>
3.1	Talin turnover is regulated by tensile force .....	36
3.2	Talin turnover regulated in response to increased force does not require integrin binding, auto-inhibition, or the talin FERM domain .....	42
3.3	Talin turnover regulation in response to reduced force requires binding through IBS1, the FERM domain, and autoinhibition .....	48
3.4	Regulation of talin turnover at the onset of muscle contractility requires physical binding to $\beta$ -integrin tails, but not activation.....	48
3.5	High temporal resolution quantification of talin turnover .....	54
3.5.1	Increased tensile force reduces talin recycling .....	55
3.5.2	Decreased tensile force does not change overall rates of talin binding or recycling.....	60
3.6	High temporal resolution quantification of tensin turnover.....	62
3.6.1	Increased tensile force increases tensin exocytosis .....	62
3.6.2	Decreased tensile force decreases overall tensin binding, and increases exocytosis.....	62
3.7	High temporal resolution quantification of ILK turnover.....	68

3.7.1	Increased tensile force increases overall ILK binding .....	68
3.7.2	Decreased force decreases ILK binding .....	68
3.8	High temporal resolution quantification of turnover throughout development .....	73
<b>Chapter 4: Discussion and Conclusion .....</b>		<b>77</b>
4.1	Force regulates talin turnover .....	77
4.2	Talin domains required for mechanotransduction .....	79
4.3	Talin domains required for developmental regulation of turnover .....	81
4.4	Mechanisms for force-mediated control of adhesion stability .....	82
4.5	Mechanisms for developmental control of adhesion stability .....	86
4.6	Conclusions .....	88
<b>Bibliography .....</b>		<b>90</b>

## List of Tables

Table 1	Mobile fraction and half-time of talin mutants in <i>Brkd</i> <sup>J29</sup> mutants .....	40
Table 2	Mobile fraction and half-time of talin mutants in <i>para</i> <sup>ts2</sup> mutants .....	41
Table 3	Mobile fraction and half-time of talin mutants during development.....	54
Table 4	Rate constants of talin turnover under increased force.....	59
Table 5	Rate constants of talin turnover under reduced force .....	59
Table 6	Rate constants of tensin turnover under increased force .....	65
Table 7	Rate constants of tensin turnover under reduced force.....	67
Table 8	Rate constants of ILK turnover under increased force .....	71
Table 9	Rate constants of ILK turnover under reduced force.....	72
Table 10	Rate constants of talin, tensin, and ILK in stage 17 embryos and 3 <sup>rd</sup> instar larvae.....	76

## List of Figures

Figure 1	Diagram of integrin and the integrin adhesion complex .....	6
Figure 2	Schematic of talin and relevant domains.....	13
Figure 3	Fluorescence recovery after photobleaching.....	24
Figure 4	Diagram of the <i>Drosophila</i> myotendinous junction (MTJ).....	29
Figure 5	Force modulates talin turnover at MTJs.....	38
Figure 6	Schematic of talin mutations used in this thesis.....	43
Figure 7	Reduction of talin turnover due to increased force does not require integrin binding, the FERM domain, or autoinhibition.....	46
Figure 8	Control of talin turnover in response to reduced force requires integrin binding through IBS1, the FERM domain, and autoinhibition.....	49
Figure 9	Downregulation of turnover at the onset of muscle activity requires binding through IBS1 .....	52
Figure 10	Characterization of the effect of force on talin dynamics .....	57
	Characterization of the effect of force on tensin dynamics .....	63
Figure 12	Characterization of the effect of force on ILK dynamics.....	69
Figure 13	Characterization of turnover regulation during development .....	74
Figure 14	Model for the effects of force on integrin adhesion complex dynamics .....	85

## List of Abbreviations

CHO – Chinese hamster ovary

ECM – Extra-cellular matrix

EGFR – Epidermal growth factor receptor

FAK – Focal adhesion kinase

FERM – 4.1 protein, ezrin, radixin, moesin

FRAP – Fluorescence recovery after photobleaching

FRET – Fluorescence resonance energy transfer

GFP – Green fluorescent protein

IAC – Integrin adhesion complex

IBS – Integrin binding site

ILK – Integrin-linked kinase

IPP – ILK PINCH Parvin

LFA-1 – Lymphocyte function-associated antigen 1 ( $\alpha$ L $\beta$ 2 integrin)

MF – Mobile fraction

MTJ – Myotendinous junction

NLLS – Non-linear least squares

PBS – Phosphate buffered saline

PIP – Phosphatidylinositol phosphate

PTB – Phosphotyrosine-binding

RGD - Tripeptide Arg-Gly-Asp motif

SH2 – Src homology 2

## **Acknowledgements**

I would like to thank my supervisor Dr. Guy Tanentzapf for supporting my research through funding and providing access to high quality equipment. Furthermore, his constructive criticism of my scientific presentations has greatly improved my ability to communicate my research, both to an audience of peers, and to a lay audience. Finally, with his guidance I have learned to better conduct independent research on a question that I helped propose, which is a skill that I hope to carry forward through life.

I would also like to thank the members of my supervisory committee, Kurt Haas and Robert Nabi, for their support and advocacy throughout my studies at UBC. They greatly helped me focus my project, and provided an important alternate point of view on my research as mentors.

Additionally, the camaraderie of all of the graduate students in our hallway constantly provided morale boosts when the going got tough. I especially thank all the current and former members of the Tanentzapf lab, and G. Stefano Brigidi and Eugenia Petoukhov from the Bamji Lab.

Last but certainly not least, I thank my family, JM, JL, LA, and AGB. You have provided so much support and encouragement to me over the years. I am so grateful.

## **Dedication**

This thesis is dedicated to my family, and the hundreds of thousands of flies who selflessly gave their lives for this scientific research.

# Chapter 1: Introduction

The ability of cells to receive and interpret signals, termed signal transduction, is vital for most, if not all, cellular functions. These functions include processes such as: proliferation, differentiation, transformation, and controlled cell death. Cells must be able to receive, integrate, and respond to external signals to ensure that the aforementioned processes occur at the correct time, and to the correct extent. Misregulation of signal transduction is responsible for a host of human diseases, from cancer, to autoimmune diseases, organ dysfunction, and developmental defects. Signal transduction is often thought of purely in the context of classical signaling involving factors such as secreted hormones and small molecules. However mechanical signals can also be converted into chemical signals by cells, a phenomenon called mechanotransduction, and this type of signaling is equally important to the types described above, and has only recently become a major focus of study. The field of mechanotransduction presents a significant opportunity for gaining important knowledge of basic biological processes, and developing solutions for human disease.

## 1.1 Mechanotransduction

Multicellular organisms can resist, sense, and adapt to a broad spectrum of mechanical forces that they encounter in nature. This necessitates physical linkages within each tissue, and within each cell, allowing cells to both withstand that force. These physical connections are also, unsurprisingly, foci for the structures that cells use to sense force, and respond appropriately to the incoming information. For example, epithelial tissues, such as skin, have keratin networks that interface through desmosomes. This adhesive process allows the entire

cell layer to be mechanically connected, and connects the ECM to actin and intermediate filaments of the cytoskeleton. Genetic mutations in many components of this interaction (especially integrin mediated adhesion proteins such as  $\alpha6\beta4$  integrin, kindlin-1, and the ECM ligands collagen VII, collagen XVII, and laminin 322) lead to mechanical fragility in epidermal tissue, leading to severe tissue blistering, worsened by trivial trauma such as friction or scratching, and can be fatal (Aumailley et al 2006).

One key feature of complex organisms is the ability to adapt to the mechanical strain acting on their tissues (Schwartz 2010). The quintessential example of this phenomenon is adjustment of muscle mass in response to exercise, with increased muscle use leading to muscle hypertrophy, and lack of use leading to atrophy (Fluck & Hoppeler 2003). This response to force is even fine-tuned based on the frequency and amplitude of force on the tissue, and controls the proportion of different muscle fiber types (type 1, 2A and 2X) that are produced due to training (D'Antona et al 2006). However there are other less obvious, but equally physiologically relevant examples, notably, arteries remodel in response to changes in fluid shear force such that vessel diameter is matched to the volume of circulating blood (Schaper 2009). Artery wall thickness is also influenced by blood pressure, with the vessel wall thickness adjusted to keep the force per unit of wall constant (Schiffrin 1992). Bone formation is another well-studied example of tissue remodeling in response to force. Both deposition of new bone and turnover of existing bone are regulated by weight-bearing activity. Bone density increases under higher loads, and decreases under lower loads (Robling et al 2006). The reoccurring theme of the aforementioned examples is one of dynamic equilibrium. This strategy ensures that resources are allocated to ensure that tissues

remain as strong as necessary to cope with the organism's environment, and changes in internal or external force. However when pushed outside of normal bounds, these regulatory mechanisms can also contribute to pathology. Muscle and bone loss is a common morbidity seen in patients on bed rest, and astronauts subject to long periods of zero gravity (Edgerton et al 1995, Leblanc et al 1990). Hypertension is a serious contributor to the risk factor for atherosclerosis and aneurysm (Hahn & Schwartz 2009, Krishna et al 2010). Ventilator associated lung injury is an acute, and serious injury for patients on ventilators, presenting as edema, bleeding, and alveolar collapse (Lionetti et al 2005).

Sensation of mechanical force is not only important for tissue homeostasis; it has a critical role in embryonic development, which has been increasingly studied in the past decade. Tissue morphogenesis during development must result in a tissue that has the correct shape, and size. Understandably, this process requires a highly complex interplay between cell adhesion, the cytoskeleton, soluble factors, and gene expression. Given that the final size and shape of organs is not encoded directly into genes, there must be other mechanisms to control morphogenesis. Numerous studies from a variety of model organisms have show that mechanical force exerted on tissue is a major determinant of the final outcome of development. During *Drosophila* embryogenesis, pressure on the anterior foregut and stomodeal primordium during germ band extension activates  $\beta$ -catenin signaling and triggers expression of mesenchymal genes such as the transcription factor *Twist* (Farge 2003). Even earlier during embryonic development, the migration of border cells from the anterior of oocyte necessitates the nuclear translocation of the transcription factor Mal-D, a process that is triggered by cellular stretching (Somogyi & Rorth 2004). More recent research on a

mammalian cardiovascular system has shown that this phenomenon is important throughout development, from early cellular movements, to specification of specific substructures of complex organs. In mouse embryos, remodeling of the yolk sac vascular plexus needs fluid shear forces from circulation (Lucitti et al 2007), and proper looping of the outflow tract from the heart also requires shear stress from outflow of blood from the heart. A classical example of a defect due to lack of fluid flow is Kartagener's syndrome, a reversal of the normal left-right patterning of the internal organs. This patterning is normally developed early in embryogenesis, by fluid flow driven by cilia. This flow is sensed by the mechanotransduction machinery of cells, and causes a differential expression of the protein nodal, leading to a signal cascade on the left side of the embryo that does not occur on the right. Mutations in the dynein family of proteins, the motors that are required for generation of fluid flow by the cilia, cause the left-right patterning to become random.

Lack of, or improper mechanical feedback not only can cause disruption of these developmental processes, but can also contribute to disease in adults. One very important example of this is; promotion of cancer progression due to changes in tissue stiffness. Tumors are much stiffer than surrounding tissue, due to increased cell proliferation, and elevated interstitial pressure. This stiffness is sensed by adhesion proteins, and leads to higher cytoskeletal tension, and a positive feedback loop, further increasing rigidity of the external environment through cellular mechanotransduction pathways. This stiffness, in breast cancer models, then leads to activation of the epidermal growth-factor receptor (EGFR) pathway, promoting tumor cell proliferation, and modulating transformation into a phenotype associated with increased malignancy (Paszek et al 2005). Conversely, if these

pathways are controlled to reduce cytoskeletal tension to normal levels, tumor cell proliferation is significantly reduced, and the malignant phenotype of cells is repressed.

## **1.2 Cell adhesion**

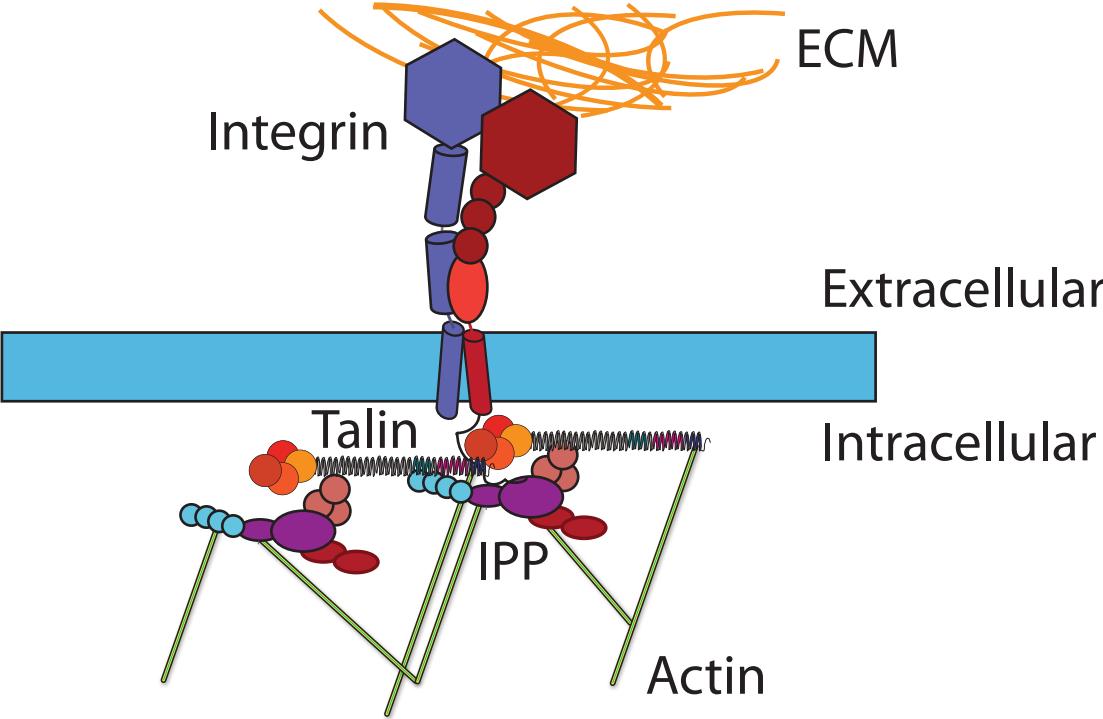
Because adhesive connections from cell-to-cell and between cells and their environment are the major ways that cells receive mechanical information from their environment, we must understand cell adhesion in order to understand mechanical signaling.

Cellular adhesion is a fundamental property of complex, multicellular life. It is required, first and foremost, to maintain the integrity of the organism. However, it is also necessary for the segregation of different types of cells, allowing for the formation of tissues and organs with specialized functions. Continued adhesion throughout the life of the animal is then required to maintain those structures. Defects that arise in cellular adhesion play a role in numerous pathologies, from neurological (Bateman et al 1996), to cardiopulmonary (Norgett et al 2000), epithelial (Pulkkinen et al 1994), and cancer (Voeller et al 1998), thus understanding cell adhesion can help us address human diseases.

There are two main types of cell adhesion, adhesion of cells to other cells (Cell-Cell adhesion), often mediated by the cadherin family of proteins, and adherence of cells to the extracellular matrix (ECM), which is a complex assembly of secreted proteins. The second type of adhesion is predominantly mediated by the highly conserved integrin family of transmembrane receptors (Fig. 1). Integrins are present in all cell types, and are required for development from *C. elegans* through mice.

**Figure 1 – Diagram of integrin and the integrin adhesion complex:** This illustration shows an integrin heterodimer with the  $\alpha$  and  $\beta$  subunits, connecting to an ECM on the exterior of the cell, and the integrin adhesion complex (IAC), which includes talin, tensin, and the ILK-PINCH-Parvin (IPP) complex, on the interior of the cell, which links integrins to the actin cytoskeleton.

Figure 1 - Diagram of integrin and the integrin adhesion complex



### 1.2.1 Integrins and the ECM

Integrin receptors function as heterodimers, composed of  $\alpha$  and  $\beta$  subunits. 18  $\alpha$  and 8  $\beta$  subunits have been characterized in mammals, which form 24 functional pairs (Hynes 2002). The extracellular domain of integrins directly bind to ECM proteins such as collagen, fibronectin, and laminin (Humphries et al 2006), this interaction occurs through highly conserved and specific recognition sequences, with one common example being the Arginine-Glycine-Aspartate (RGD) motif, which is conserved in fibrinogen, fibronectin, tigrin, and vitronectin. The ECM protein composition of different matrices can vary widely, and each heterodimeric combination of  $\alpha$  and  $\beta$  subunits has affinity for a distinct subset of ECM types, with some overlap between different pairs. For example,  $\alpha1\beta1$ ,  $\alpha2\beta1$ ,  $\alpha10\beta1$ , and  $\alpha11\beta1$  all have high affinity for collagen, which is the main component of human connective tissue. The heterodimers  $\alpha3\beta1$ ,  $\alpha6\beta1$ ,  $\alpha6\beta4$ , and  $\alpha7\beta1$ , on the other hand, are classical binding partners for laminin, the major component of basal lamina (Geiger & Yamada 2011). In addition, some ECM proteins have multiple splice variants that drastically alter the molecule, for example certain laminin isoforms have an RGD motif that is not recognized by laminin binding integrins, and in others the motif is only exposed upon denaturation or proteolytic cleavage (Barczyk et al 2010).

This complexity, and redundancy, of integrin-mediated adhesion in mammals makes *in vivo* investigations challenging. However, because basic integrin structure and function are highly conserved throughout evolution, the invertebrate model organisms, *Caenorhabditis elegans* and *Drosophila melanogaster* provide an excellent way to decipher the intricacies of cell-ECM adhesion and the specifics of integrin function in numerous biological processes. These

organisms have fewer integrin heterodimer pairs, and less redundancy of adhesion within tissue.

The *Drosophila* genome contains five  $\alpha$  ( $\alpha$ PS1-5) and two  $\beta$  ( $\beta$ PS and  $\beta$ v) subunits (Brower 2003).  $\alpha$ PS1, first named because of its “position specific” expression pattern on the dorsal side of the wing disc epithelium, is a typical laminin-binding type of  $\alpha$  subunit, similar to  $\alpha$ 3,  $\alpha$ 6, and  $\alpha$ 7 in mammals.  $\alpha$ PS2 was first noted for its position specific expression on the ventral side of the wing disc, and is similar to the RGD binding mammalian integrins  $\alpha$ IIb,  $\alpha$ V,  $\alpha$ 5, and  $\alpha$ 8 (Wilcox et al 1981). The three remaining  $\alpha$  subunits lack obvious vertebrate orthologs but do play important roles in development and adult life (Adams et al 2000, Stark et al 1997). Mutations in both  $\beta$  subunits have been described, and have shown that  $\beta$ PS integrin is the primary  $\beta$  subunit, with  $\beta$ v only being expressed in the midgut, and functionally redundant with  $\beta$ PS. Because there are only two  $\beta$  integrin subunits, it is possible to study the effects of complete loss of integrin during development. Loss-of-function mutations in the *myospheroid* gene, which encodes  $\beta$ PS, are lethal, and cause severe defects during embryogenesis, affecting multiple morphogenetic tissue movements, and disrupting muscle adhesion, which causes the muscles to detach and round up (Wright 1960).

### **1.3 The integrin adhesion complex**

On the interior of the cell membrane, most integrins connect to actin through a network of IAC proteins consisting of over 180 components, with over 800 interactions (Zaidel-Bar & Geiger 2010, Zaidel-Bar et al 2007). The one exception is vertebrate  $\alpha$ 6 $\beta$ 4, which links its ligand laminin to intermediate filaments, through the cytolinker plectin. The composition and

stoichiometry can vary widely depending on the type of Integrin-mediated adhesion. Numerous IAC components can link integrins to actin filaments, including talin, tensin, vinculin,  $\alpha$ -actinin, filamin, melusin, skelemin and parvin (Brancaccio et al 1999, Burridge & Connell 1983a, Burridge & Connell 1983b, Heggeness et al 1977, Le Clainche et al 2010, Nikolopoulos & Turner 2000, Price 1987, Wehland et al 1979, Wilkins et al 1986). Examples of other important IAC proteins include Integrin-Linked Kinase (ILK), Focal Adhesion Kinase (FAK), Src family kinases, paxillin, kindlin, PINCH, Wech, and others (Golden et al 1986, Hannigan et al 1996, Huang et al 1991, Kloeker et al 2004, Loer et al 2008, Pestina et al 1997, Rendu et al 1989, Schaller et al 1992, Tu et al 1999, Turner et al 1990, Zaidel-Bar et al 2007).

In *Drosophila*, forward genetics screens have led to the identification and characterization of mutations in more than a dozen genes that encode intracellular components of integrin adhesions. These include orthologs of talin, PINCH, ILK, vinculin, FAK, paxillin, and tensin. Some phenotypes of these mutants mirror loss of function *myspheroid* mutants. However, others only affect a subset of integrin-mediated adhesion, and some have no phenotype, indicating compensatory factors that preserve adhesion. This observation demonstrates two facts: (1) some components have a vital role in the adhesion complex, whereas others play a more minor role, and (2) integrin adhesion is not a simple linear pathway. Similar to mammalian systems, talin forms a core complex with integrin in flies as well. Downstream of that complex, the pathway branches, such that some proteins, including ILK and PINCH, are partially redundant. Other integrin associated proteins such as tensin, vinculin, FAK, and paxillin have a weak, or wildtype phenotype.

The availability of knowledge, and the simplification of the integrin system (while still maintaining conservation) make *Drosophila* a powerful model system for the study of integrin function. Furthermore, the availability of tools such as: tissue specific control of protein expression, antibodies, mutants, transgenic constructs, and antibodies allows the investigation of biological questions that would be nearly impossible in mammalian systems. Finally, fly embryos and larvae are clear, meaning that it is possible to visualize integrin adhesions in an intact, living organism, using fluorescent proteins.

For the purpose of my project, we chose three intracellular protein components, at different levels in the pathway of integrin-mediated adhesion, as the focus of study. These proteins were talin, tensin, and integrin-linked kinase.

### *1.3.1 Talin*

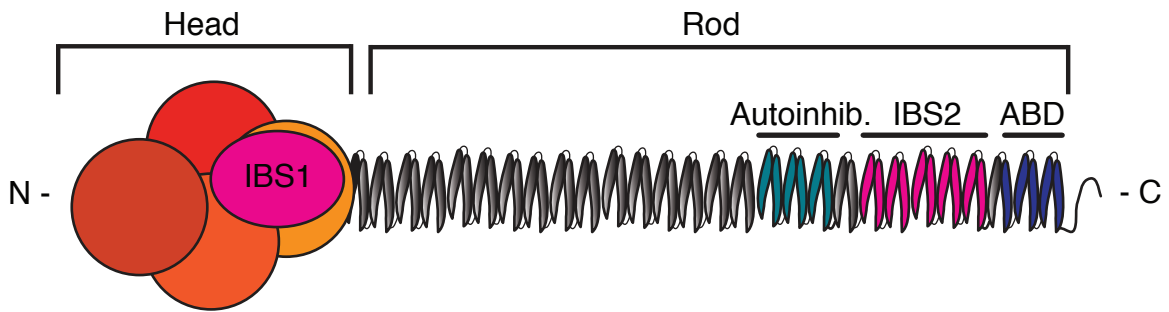
Talin is an essential linker between integrin and the IAC, and was the first cytoplasmic protein shown to bind the intracellular domain of integrins (Burrige & Connell 1983a). However talin has many important functions within the IAC in addition to that of a structural cytolinker. Binding of talin to the tail of  $\beta$ -integrin has a key role in integrin activation, inducing a conformational change in the extracellular domain of the integrin heterodimer, thereby increasing its affinity for ECM ligands (Calderwood 2004, Ginsberg et al 2005, Tadokoro et al 2003).

Structurally, talin is a large (~270 kDa) protein, with a head domain and a flexible rod domain of 62 repeating alpha helices (Fig. 2). The globular head region contains a FERM (band 4.1, ezrin, radixin, moesin) domain (further divided into F1, F2, and F3 subdomains). The FERM domain contains one binding site for the cytoplasmic tail of  $\beta$ -integrins, which binds with high affinity to the cytoplasmic tails of integrin subunits  $\beta$ 1,  $\beta$ 2,  $\beta$ 3 and  $\beta$ 5 (Critchley & Gingras 2008). The head domain also binds signaling proteins that regulate the dynamics of focal adhesions. These include PIPK1 $\gamma$ 90 [a splice variant of phosphatidylinositol (4)-phosphate 5-kinase type I $\gamma$ ], focal adhesion kinase (FAK), and the hyaluronan receptor layilin (Borowsky & Hynes 1998, Critchley & Gingras 2008). The head region also contains one motif that binds actin. The talin rod region contains one integrin-binding site (that we term IBS2 in this thesis), numerous actin binding sites (two of which are characterized), and several binding sites for vinculin, which itself binds multiple further proteins. In focal adhesions, talin functions as a dimer, although the relative position of the two subunits within the dimer is uncertain.

In both mammalian and fly systems, talin has been shown to play a central role in the beginning of focal complex and adhesion assembly upon binding of integrin to the ECM. Also, talin degradation has an important role in focal adhesion turnover (Franco et al 2004). Vertebrates have two genes that encode closely related talin proteins (74% identity). Disruption of the *Tln1* gene in mice is lethal during early embryonic development, caused by arrested gastrulation (Monkley et al 2000). However, mice that are homozygous for a *Tln2* gene-trap allele are viable (Chen & Lo 2005). Because of the early lethality of talin-1

**Figure 2 – Schematic of talin and relevant domains:** Talin is composed of two general regions. The N-terminal head, which contains the F0 subdomain and the FERM domain, is composed of the F1, F2, and F3 subdomains. The FERM domain contains 1 actin-binding site, interaction sites for FAK, and PIP kinase, and the F3 subdomain contains the first integrin-binding site. The C-terminal rod is the second region, and is composed of repeating amphipathic helices. The rod contains two actin-binding sites, the best characterized of which resides close to the C-terminal end of the protein. It also contains numerous vinculin-binding sites that can be exposed by tensile force, and a region that can bind to a complementary region in the head, inhibiting talin function, including integrin binding. Insect talin contains a short additional unstructured C-terminal region.

**Figure 2 – Schematic of talin and relevant domains**



deficient mice, and the presence of two isoforms, much of the research on talin function is done with *in vitro* cell culture experiments, or model organisms such as *Drosophila*.

Defects seen upon loss of talin have helped elucidate the key role of talin in development and in normal cellular function. Embryonic stem cells lacking talin-1 do not spread on collagen or laminin; however, these cells can spread on fibronectin, but cannot assemble vinculin- or paxillin-containing focal adhesions, or actin stress fibers (Zhang et al 2008). Talin knockdown in CHO cells was shown to inhibit activation of integrin  $\alpha$ IIb $\beta$ 3,  $\alpha$ V $\beta$ 3 and  $\alpha$ 5 $\beta$ 11 (Tadokoro et al 2003), and overexpression of the N-terminal talin head domain leads to a significant increase in integrin  $\alpha$ IIb $\beta$ 3 activation in CHO cells (Calderwood et al 1999). Talin was identified as the important component for maintaining a 2 pN slip bond between fibronectin and the cytoskeleton using optical tweezers to obtain force measurements, and evidence indicates that talin is required for integrin mediated force generation events (Jiang et al 2003). In *Drosophila*, there is only one gene, *rhea*, which encodes talin. In the fly, functional talin is not required for integrin localization to cell surfaces or myotendinous junctions (MTJs), however it is necessary for the assembly of focal-adhesion like structures in imaginal disc epithelia, and the formation of junctions between the muscle and tension cells. Embryos that lack talin phenocopy  $\beta$ PS null embryos, and have defects in early morphogenetic movements such as germ band retraction, dorsal closure, and lack stable muscle attachments (Brown et al 2002). Unlike vertebrate talin, *Drosophila* talin is necessary *in vivo*, but not sufficient using *in vitro* assays, for integrin functionality. Disrupting integrin binding using talin with a single point mutation in the head region (R367A) does not fully rescue talin deletion, and results in dissociation of integrins from the ECM. However direct

measurements of integrin activation using an *in vitro* assay show that neither *Drosophila* nor mammalian talin activate the *Drosophila* integrin  $\alpha$ PS2 $\beta$ PS due to structural differences in the extracellular and/or transmembrane domain (Helsten et al 2008, Tanentzapf & Brown 2006). Recently, new techniques have allowed the study of talin in vertebrates *in vivo*. Using a conditional *Tln1* allele, studies demonstrated for the first time that talin-1 is necessary for the activation of platelet integrins  $\alpha$ 2 $\beta$ 1 and  $\alpha$ IIB $\beta$ 3 *in vivo*, and the mutant mice exhibit spontaneous bleeding (Nieswandt et al 2007, Petrich et al 2007).

### 1.3.2 Tensin

Tensin is another important component of the integrin-mediated adhesion. Tensin, similarly to talin, is a large protein, with approximate molecular weight of 220 kDa, and which functions as a structural and signaling scaffold (Lo 2004, Torgler et al 2004). Tensin also contains a number of conserved domains with well-described function. Firstly, there are multiple actin binding sites that allow for capping of the barbed ends of actin filaments and for the crosslinkage of filaments, while promoting actin aggregation (Lo et al 1994). Tensin is also known to bind PI3K, p130Cas, and FAK through its Src Homology 2 (SH2) domain (Davis et al 1991, Lo 2004). This interaction through the SH2 domain causes tensin to be recruited to sites of high tyrosine kinase activity. Finally, tensin can interact with asparagine-x-x-tyrosine (NxxY) motifs on  $\beta$ -integrin tails through a phospho-tyrosine binding (PTB) domain (Calderwood et al 2003, Torgler et al 2004). Tensin appears to have a role in mature integrin adhesions. It was shown to co-localize with clustered integrin, and is phosphorylated in response to integrin activation ((Bockholt & Burridge 1993, Miyamoto et al 1995a, Miyamoto et al 1995b). The distribution of tensin in fibroblasts also shows enrichment in

mature fibrillar integrin adhesions, and expression of a tensin fragment inhibits fibrillar adhesion to fibronectin (Pankov et al 2000, Zamir et al 1999). Although tensin has a clear role in integrin-mediated adhesion, tensin null mutations in mice and flies are viable. However, tensin is important for stabilizing integrin adhesions in the kidney, and enabling normal repair of muscular damage. Null mutants in *Drosophila* are also only deficient in a small subset of integrin-mediated adhesion, in the wing epithelial tissue (Lo 2004, Torgler et al 2004).

### *1.3.3 Integrin-linked kinase*

Integrin-linked kinase is another vital component of integrin signaling (Hannigan et al 1996, Legate et al 2006). As with talin, ILK is an essential cytolinker and functions as a signaling scaffold in the IAC. ILK functions as a hetero-trimeric complex with the proteins PINCH (a LIM domain protein), and parvin (a paxillin and actin binding protein). This important signaling scaffold, termed the IPP complex, is required in mammals for the targeting of focal adhesion proteins to sites of integrin-mediated adhesion (Legate et al 2006). Structurally, ILK has an N-terminal ankyrin repeat domain, through which binding to PINCH occurs. The C-terminal region contains the kinase domain that mediates binding to parvin, paxillin, and  $\beta$ -integrin cytoplasmic tails (Hannigan et al 2005, Legate et al 2006).

Although the protein is named as a kinase, the kinase domain region of ILK lacks the catalytic residues that are normally conserved among protein kinases, and whether or not ILK has kinase activity is controversial (Hannigan et al 2005, Legate et al 2006). ILK's role in integrin signaling and cytoskeletal connections, however, is well studied. Relevant to our

investigation, this signaling role is conserved from invertebrates to mammals. Unlike many other focal adhesion proteins, such as FAK, there are only a few structural observations available for ILK. Like talin, ILK also genetically interacts with kindlin proteins (Mackinnon et al 2002). It is thought that this interaction might account for the results that implicate ILK in integrin activation (Tucker et al 2008).

ILK's kinase domain has been shown to play a role in integrin binding. ILK contains three ankyrin repeats in the N-terminal region of the protein, followed by a linker PH domain. The predicted kinase domain in the C-terminus is shown to mediate direct ILK binding to the cytoplasmic tails of  $\beta 1$  and  $\beta 3$  integrin (Hannigan et al 1996, Pasquet et al 2002). A majority of the other characterized binding partners of ILK also interact through the C-terminus region.

Knockout studies of ILK and PINCH have implicated them in cell-ECM adhesion formation and turnover, and in cytoskeletal organization. Deletion of the *ilk* gene in mice leads to early embryonic lethality, and fibroblasts lacking ILK have significantly impaired adhesion to ECM ligands, including fibronectin, vitronectin and laminin (Sakai et al 2003). Total inhibition of ILK has shown that the protein is required for eukaryotic development. Genetic knockout studies have shown a lack of ILK prevents the recruitment of F-actin to the plasma membrane at muscle attachment sites (Mackinnon et al 2002). These loss-of-function studies show the major role that ILK plays in protein-protein interaction, cytoskeletal organization, and signaling cascades. In addition, embryonic lethality due to serious and multiple defects, such as cardiac and skeletal muscle dysfunction, was observed in other model systems,

including *Xenopus laevis*, zebrafish, and *Drosophila melanogaster* (Knoll et al 2007, Sakai et al 2003, Zervas et al 2001).

## **1.4 Integrins as mechanosensors**

### *1.4.1 Integrin directly responds to force*

Increasingly, studies are demonstrating evidence that integrins themselves act as mechanosensors, transducing force originating on the interior and exterior of the cell membrane. The primary response of integrin adhesions to mechanical force is strengthening or reinforcement, a phenomenon called a ‘catch bond’. In migrating cells, adhesions enlarge and recruit new cytoskeletal proteins in order to resist the forces endured during migration and cellular contractility. Force is even a requirement for adhesion maturation; focal adhesions do not develop from focal contacts unless connected to highly contractile actin stress fibers, and when they are treated with myosin inhibitors like blebbistatin, they disassemble rapidly (Chrzanowska-Wodnicka & Burridge 1996). Less mature integrin adhesions, focal complexes, which are not associated with large actin stress fibers, are also dependent on functional myosin (Choi et al 2008). These focal complexes develop from even smaller, nascent adhesions, but only if they connect to the cellular acto-myosin network, and focal complexes devolve into nascent adhesions when myosin inhibitors are applied. Alterations in adhesion maturity and size occur rapidly after altering forces, on the timescale of seconds or minutes. The timescale of these changes indicate that efficient control mechanisms are in place beyond classical signaling (Balaban et al 2001).

Integrins themselves undergo complex conformational rearrangements due to internal or external signals that, and these changes govern both affinity for extracellular matrix proteins and associations with cytoskeletal proteins (Calvete 2004, Campbell & Humphries 2011, Wegener & Campbell 2008). It is therefore likely that these conformations are also sensitive to mechanical signals from extracellular ligand binding, and to binding of the cytoplasmic complex to integrin cytoplasmic domains. Indeed, experimental data support the idea that integrin conformation can be modulated by applied force (Friedland et al 2009, Puklin-Faucher et al 2006).

One classical example of integrins as mechanotransducers comes from the heart. Contractions of the heart create a high magnitude of mechanical force, and integrin mediated signaling is required for the ability of cardiomyocytes to adapt to those forces. Also, integrins are thought to play a role in changes in cardiac function due to tissue remodeling after myocardial infarction, and during heart failure. Another study of adhesion through leukocyte integrin LFA-1 ( $\alpha$ L $\beta$ 2) also suggests that force can regulate integrin conformation, indicating that strain induced conformational changes are a general mechanism for regulating many types of integrin (Jin et al 2004, Zhu et al 2008). Tension applied to cells on elastic surfaces also results in an increase in integrin affinity as measured by binding of soluble FN fragments (Katsumi et al 2005, Thodeti et al 2009). One interpretation of these results is that communication from the load-bearing bound integrins to the unbound integrins converts the unbound receptors to a high affinity state, causing enlargement of adhesions (called integrin clustering). This signal is mediated in a PI3K dependent manner (Katsumi et al 2005).

In *Drosophila*, Pines and colleagues used conditional mutants to alter force on integrin adhesions, and combined that with imaging experiments and mathematical modeling, finding that mechanical force directly modulates integrin adhesion dynamics *in vivo* at sites of stable adhesion between muscles and tendons (Pines et al 2012). Furthermore, we showed that point mutants in the  $\beta$ -integrin subunit that are known to disrupt conformational changes in integrin induced by the ECM, or downstream signaling through integrins abrogate this effect. When force is increased at adhesive sites, inside-out signaling via the proximal NPxY motif in integrin tails, and outside-in signaling through extracellular integrin conformational changes, stabilize adhesive foci by reducing the rate of integrin removal from the membrane. This reduces the percentage of integrins that are mobile at the membrane. When force is reduced, the inside-out signaling through both NPxY motifs and tyrosine phosphorylation, and outside-in signaling via conformational changes, increase both the rate of endocytosis and exocytosis, although the portion of mobile integrins does not change.

#### *1.4.2 The integrin adhesion complex is also directly modulated by force*

On the interior of the cell, the IAC and the adhesion-associated actin cytoskeleton rapidly remodel in response to changes in force; the best studied case being adhesion reinforcement, or, strengthening. Experiments with optical tweezers showed that adhesions begin to recruit vinculin and increase their strength within seconds of applying force (Galbraith et al 2002). This vinculin recruitment is now known to be caused by cryptic vinculin-binding sites in the talin tail domain, which are normally concealed within bundles of  $\alpha$  helices, and which open under tension (Campbell & Humphries 2011, del Rio et al 2009). However in *Drosophila*, vinculin mutants have no phenotype, leaving open the possibility that one of the many other

protein-protein interactions through talin may also be an important part of force-transduction through the IAC.

Integrin adhesions however, do not always strengthen under force. In order for cells to successfully migrate, they need to also disassemble adhesions under certain amounts of force (Ballestrem et al 2001). Recent studies have investigated the mechanism responsible for force dependent adhesion disassembly. The creation of a fluorescence resonance energy transfer (FRET) tension sensor for vinculin showed that high force applied to that protein causes an increase in vinculin recruitment, which then reduces the force across each individual vinculin molecule (Grashoff et al 2010). However, along the trailing edge of the migrating cell, there was a population of focal adhesions where applied force across vinculin was negligible. These adhesions translocate towards the center of the cell in a type of controlled disassembly called centripetal sliding (Ballestrem et al 2001).

In addition to the investigation of integrin turnover *in vivo*, and using the same techniques discussed previously, the effect of force on the IAC components ILK and tensin has also been investigated, by visualizing the mobility of these components using temperature-sensitive mutants with altered muscle contractility. Results showed that force has an inverse relationship with tensin and ILK mobility, however methodological difficulties prevented the identification of the molecular mechanism for this.

## 1.5 Integrin turnover

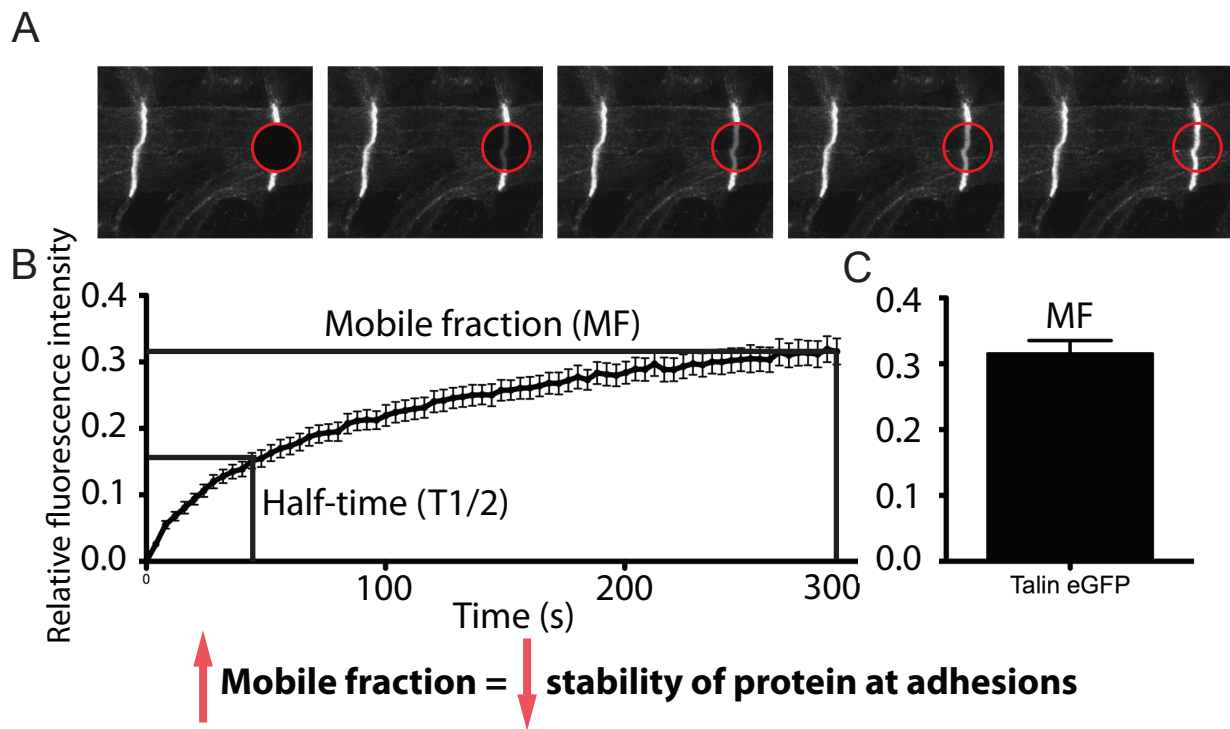
### 1.5.1 *Fluorescence recovery after photobleaching*

For previous work investigating integrin and IAC turnover *in vivo*, and this current project, Fluorescence Recovery After Photobleaching (FRAP) is the method of choice (Fig. 3). FRAP is a technique that was developed in the 1970s as a tool to investigate molecular mobility in different media (Peters et al 1974). Cell biologists modified the technique to study membrane diffusion of lipids and fluorophore-coupled proteins (Axelrod et al 1976, Edidin et al 1976). More recently, the development of non-invasive fluorescent tags, such as Green Fluorescent Protein (GFP), has allowed the study of molecular movement within living cells (Reits & Neefjes 2001). A FRAP experiment involves briefly exposing a target region/organelle/membrane of a cell with a high-intensity laser. This illumination causes an irreversible loss of fluorescence in the area, called photobleaching. As molecules with fluorophores from outside of the photobleached area begin to move into the dark region, there is a measureable recovery of fluorescence. From that recovery, it is possible to calculate the percentage of molecules that are mobile in the region of interest (mobile fraction; MF), and coefficients for the rate of recovery (Braga et al 2004).

There are two prevailing models for transmembrane protein turnover: (1) passive lateral diffusion of proteins within the membrane, and (2) active endocytic/exocytic cycling of proteins (Kusumi et al 1993, Sorkin & von Zastrow 2009). FRAP was used in cell culture to show that integrins are highly mobile at sites of transient adhesion in migrating cells (Ballestrem et al 2001), and there is evidence that both passive and active mechanisms are responsible for integrin mobility in that system (Caswell et al 2009, Wehrle-Haller 2007),

**Figure 3 – Fluorescence recovery after photobleaching:** (a) Fluorescently-tagged protein shows dense localization to MTJs. This fluorescence is bleached using a high-intensity laser, and fluorescence recovery is (a) recorded over 300 seconds, and (b) quantified. The data is used to produce a curve showing the pattern of recovery over time (b), and the calculated recovery plateau is used to estimate the final overall mobility of the protein (c).

**Figure 3 – Fluorescence recovery after photobleaching**



however work from our lab has shown that lateral diffusion does not play a major role in integrin dynamics, *in vivo*, at stable adhesive sites (Yuan et al 2010).

### *1.5.2 Integrin adhesion disassembly and recycling*

Most of the current body of knowledge concerning the de-construction of integrin adhesions comes from studies on polarized cell migration, as this process is known to require adhesion disassembly. Chinese Hamster Ovary (CHO) cells were first used to show that integrins are endocytosed into the cytoplasm, and then returned to the plasma membrane through recycling and exocytosis (Bretscher 1989, Bretscher 1992). Towards the rear of the cell, disassembly of integrin-mediated adhesions at the rear controls detachment of the tail of the cell, which allows for movement of the cell body forward (Broussard et al 2008, Parsons et al 2010, Webb et al 2002). Internalization of integrins can occur through clathrin- or caveolin-dependent pathways, and also through the internalization of lipid rafts (Ezratty et al 2009, Mosesson et al 2008, Pellinen et al 2006), and can be recycled via numerous different methods (Caswell & Norman 2006, Ezratty et al 2009, Pellinen & Ivaska 2006). In the fly, integrin is recycled via clathrin-dependent endocytosis, and requires Rab5 (Yuan et al 2010). Less is known about the dynamics of integrins and the adhesion complex in stable adhesions, such as muscle attachments. However, two studies from our lab showed that surprisingly, maintenance of integrin adhesion during adult life, and integrin recycling are both required for functional musculature in *Drosophila* (Perkins et al 2010, Yuan et al 2010).

### *1.5.3 Integrin adhesion complex disassembly*

Although control of adhesion disassembly in the IAC is less well understood than integrin turnover, the following characteristics of disassembly have been demonstrated. Protein cleavage by calcium-dependent proteases of the calpain family plays a major role in integrin adhesion disassembly (Dourdin et al 2001, Huttenlocher et al 1997). Calpains are known to cleave a number of vital components of integrin adhesions, notably talin, paxillin, and FAK (Carragher et al 1999, Franco & Huttenlocher 2005, Franco et al 2004, Glading et al 2002). The cleavage by calpain leads to adhesion disassembly, and inhibition of this process adversely affects cell migration. Additionally, calpain-mediated cleavage of talin and FAK are known to be rate-limiting steps of focal adhesion turnover (Chen et al 2010, Franco et al 2004). However calpain has not been shown to cleave talin in *Drosophila*.

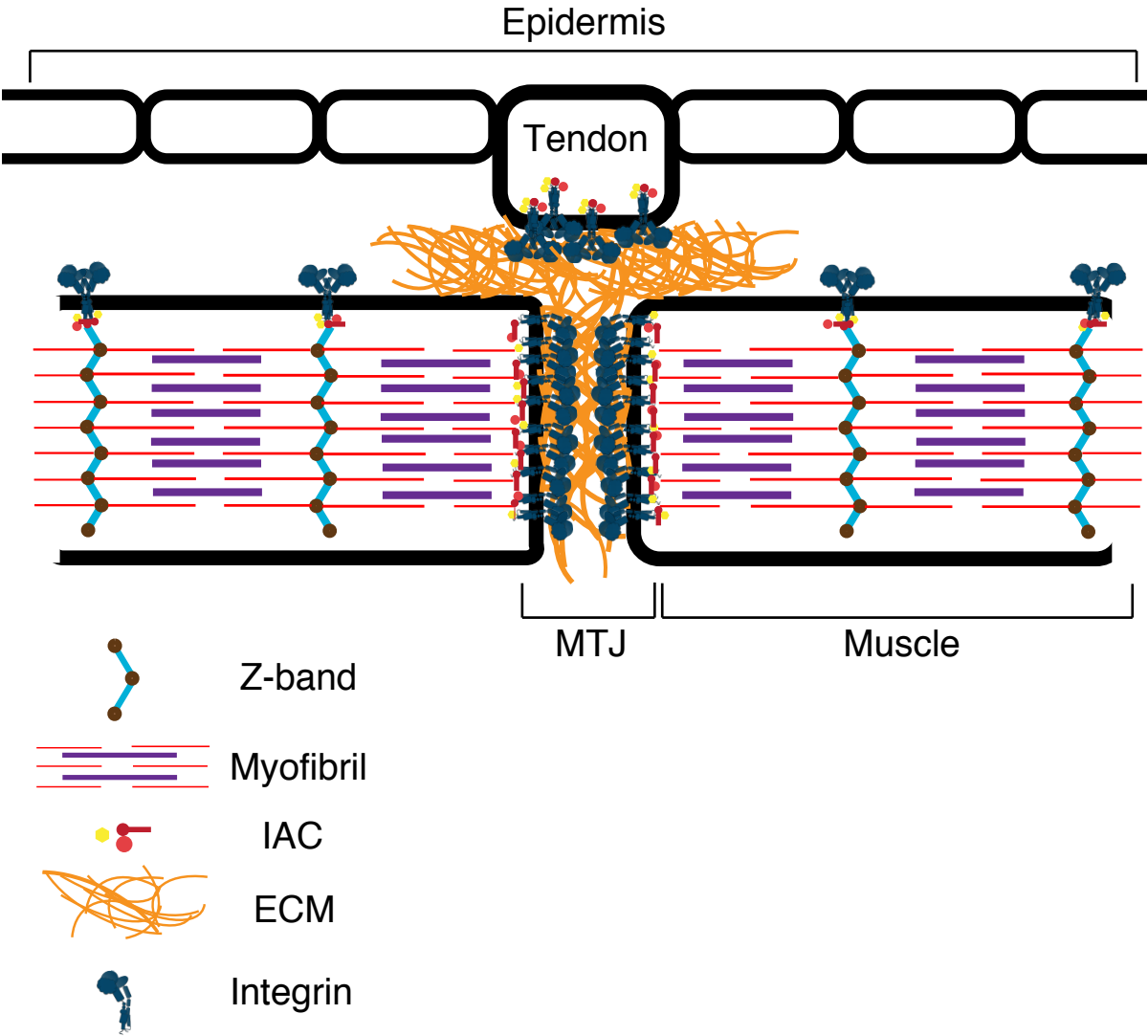
## **1.6 Objectives, rationale, hypothesis**

Despite the importance of integrins, very little is known about the process of stable adhesion turnover *in vivo*. The dynamics of integrin-mediated adhesion are well studied in cell culture, which is informative for the role of transient cell-ECM adhesion in processes such as cell migration, immune response and wound healing. Stable integrin adhesions, on the other hand, are required for the maintenance of muscles and the basement membrane. In addition, cell-ECM adhesions are known to be important foci for mechanotransduction, with talin acting as a key component. However, distinct mechanisms for mechanotransduction *in vivo* are lacking. Investigation of cell-ECM adhesion is often conducted *in vitro*, as it allows for advanced imaging studies of the structure and dynamics of adhesions. Obstacles such as tissue depth, animal movement, and invasiveness of the experimental procedures hamper advanced *in vivo* imaging of mammalian systems, such as mice. In spite of this, protocols

have been developed for confocal imaging of the circulatory systems, skeletal systems, and neural tissue. Although feasible in mammalian systems, confocal techniques require anesthesia, which arrests muscle contractions. The use of the *Drosophila* larval myotendinous junction (MTJ) (Fig. 4) as a model for stable cell-ECM adhesion allows the

**Figure 4 – Diagram of the *Drosophila* myotendinous junction:** MTJs are a well-established model for stable integrin adhesion. At MTJs, tendon and muscle cells attach to a tigrin-based ECM secreted by tendon cells. In muscles the integrin heterodimers are attached to the actin structure of myofibrils.

Figure 4 – Diagram of the *Drosophila* myotendinous junction (MTJ)



study of this process in whole, intact organisms using confocal imaging, without anesthesia, which is impossible in a mammalian system. As well, the multitude of genetic tools available for the study of *Drosophila* (such as stock centers with mutants, RNAi libraries), and the speed of organismal development allow us to perform this research in a cost-effective and time-efficient manner. Generally the human homologs of *Drosophila* genes are well conserved, and talin is especially well conserved. Approximately 50% of the amino acids in *Drosophila* Talin are identical to the corresponding residue in human isoforms, with specific domains having an even higher level of conservation. This means that the results from our experiments will not only provide knowledge of a basic cell biological process, but also be relevant to investigations in mammals.

To better understand how force modulates the IAC we have undertaken two experiments: (1) determine the effect of tensile force generated by the muscle on talin, tensin and ILK turnover using a new FRAP protocol, and (2) determine the specific protein-protein interactions that regulate talin turnover during embryonic and larval development, and in response to mechanical force.

The work presented in this thesis will provide detailed mechanistic insight into the dynamics of Integrin-based adhesion, and may contribute to our understanding of how cell adhesion processes are modulated over the course of development and throughout the life of the organism.

## Chapter 2: Materials and Methods

### 2.1 Fly stocks

Generation of *pUbi-Talin:GFP* IBS1 and IBS2 mutants is previously described (Ellis et al 2011), and *pUbi-Talin:GFP* L334R, and E1777A mutants were based on the full-length *pUbi-Talin[EGFP]*(Yuan et al 2010) and were created as described previously (Ellis *et al* 2010). The *ILK::GFP* and *blistery::GFP* genomic construct are previously described (Hudson et al 2008, Torgler et al 2004). The lines used for force modulation, *Brkd<sup>J29</sup>/TM3*, and *para<sup>ts2</sup>*, were gifts from J. Troy Littleton, and are previously described (Montana & Littleton 2004). Animals used for FRAP experiments were heterozygous for each fluorescent transgene and either *Brkd<sup>J29</sup>* (stage 17 embryos) or *para<sup>ts2</sup>* (3<sup>rd</sup> instar larvae). Stage 17 embryos were used for the induction of the *Brkd<sup>J29</sup>* phenotype as we found the most pronounced effect of hypercontractility on protein dynamics at this stage of development. Third instar larvae were used for experiments simulating reduced force because the *para<sup>ts2</sup>* phenotype presents at this stage. Specific genotypes for each FRAP experiment are described in Chapter 3.

### 2.2 FRAP experiments and statistical analysis

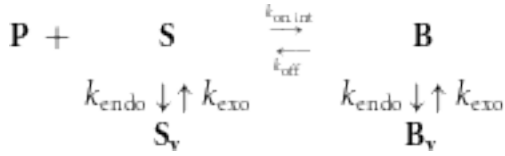
FRAP experiments were performed on intact embryos and larvae two hours after mounting on glass slides in PBS. Animals used for these experiments were aged to the correct stage and collected from apple juice agar plates, and washed in phosphate buffered saline (PBS). Embryos were dechorionated in 50% bleach for 3 minutes and re-washed in PBS before mounting, larvae were mounted directly after the first wash. MTJs from a mixed population

of the dorsal muscles DO1/DO2 and DA1/DA2, and ventral-longitudinal muscles VL1-4 were used in order to minimize the small variations in basal protein turnover rates that exist between different muscle types (Pines et al 2012). Any muscles that showed defects or tearing were excluded. For the force modulation experiments using *Brkd<sup>129</sup>* and *para<sup>ts2</sup>*, larvae were placed at 37°C for 2 hours immediately after mounting, before FRAP experiments were performed. A Tokai Hit stagetop incubator (Tokai Hit Ltd, Japan) was used to maintain temperature during experiments where necessary. FRAP was conducted using an inverted confocal microscope (Olympus Fluoview FV1000) using UplanSApo 60X/1.35 oil objective (Olympus). MTJs were photobleached using a 405nm laser at 30% power for 2 seconds causing at least a three-fold reduction in the initial fluorescence intensity, and the subsequent recovery was recorded using a 473nm laser at 2% power. For the experiments with Talin mutants, the recovery was quantified every 4 seconds for 5 minutes. For the high-time resolution experiments, recovery was quantified using three different protocols; quantification every 4 seconds for 5 minutes, quantification every 0.8 seconds for 188 seconds, and quantification every 0.4 seconds for 32 seconds. This allowed us to increase the fidelity of our mathematical models.

### **2.3 Mathematical modeling of IAC protein dynamics**

To calculate the rate constants discussed in this thesis, we derived a theoretical model to simulate the mechanisms that underlie IAC dynamics at integrin adhesions. This model accounts for binding, unbinding with integrins or the adhesion complex at the membrane, as well as recycling of the proteins while bound to integrins during endocytosis. The recovery, termed  $f(t)$ , is calculated using two linked ordinary differential equations, for a total of four

independent parameters.  $k_{endo}$  and  $k_{exo}$  which measure the rates of endocytosis and exocytosis of integrin with bound the bound IAC protein, and  $k_{on}$  and  $k_{off}$  which are the kinetics of binding and unbinding of the cytosolic protein to integrins or the adhesion complex:



This model represents 3 compartments of proteins. The fluorescently labeled protein P binds to an unlabeled membrane-localized

substrate S, forming a bound complex B. Both S and B can be internalized from the membrane, and recycled back to it. In order to fit our FRAP results to this model, we assume that the endocytosed compartment isn't accessible to the cytoplasmic pool of proteins. We also assume that the rate of endocytosis and exocytosis are identical for both S and B. Finally, we assume that the system is at an equilibrium state before photobleaching, and photobleaching reduces only P to 0. Incorporating these assumptions into our model, we arrive at:

$$\begin{aligned}
 \frac{df}{dt} &= [k_{off} + (k_{endo}/k_{exo})k_{on}] - (k_{on} + k_{off} + k_{endo})f(t) + (k_{exo} - k_{on})v(t) \\
 \frac{dv}{dt} &= k_{endo}f(t) - k_{exo}v(t) \quad \text{with the initial conditions: } f(0) = 0 \quad \text{and} \quad v(0) = k_{endo}/k_{exo}
 \end{aligned}$$

We then used a nonlinear least squares (NLLS) minimization scheme with the Levenberg-Marquardt algorithm (Press 2007) to solve this system and fit the collected FRAP data to these models, and a numerical integrator in order to solve the system of ordinary differential equations. All of the individual FRAP experiments were fit simultaneously. For each calculated fit, we used bootstrap resampling of residuals to generate  $\geq 1000$  bootstrap replicates, and fit these, in order to create bootstrap distributions for the model parameters (Pines et al 2012). The error values and significance were calculated using the bootstrap

distributions, which involves. A Bonferroni correction of significance level was used to account for multiple comparisons between two datasets (Wasserman 2004). Computations were performed using custom Python code, with the SciPy library.

## Chapter 3: Results

### 3.1 Talin turnover is regulated by tensile force

To test whether tensile force regulates talin dynamics *in vivo*, I used well-established, temperature-sensitive mutations that affect neuronal activity, to induce both an increase and decrease in muscle contractility. This allowed the alteration of tensile force in a controlled manner, in the context of an intact, living organism, by raising the temperature of the animal from 25°C to 37°C. Using the organism's own muscles also ensures that the change in force is physiologically relevant. To increase muscle contractility, I used a temperature sensitive mutation in the *Breakdance* gene (*Brkd*; allele *Brkd<sup>J29</sup>*). The exact nature of this mutation is not known, but mutant animals exhibit normal muscle physiology and contraction behavior at 25°C, however at 37°C, neuronal activity causes seizure-like hypercontraction of the muscles (Montana & Littleton 2004). To reduce muscle contractility I used a temperature-sensitive mutation of the gene *paralytic* (*para*; allele *para<sup>ts2</sup>*), which encodes a voltage-gated sodium channel. This mutation also exhibits normal muscle physiology and contraction behavior at 25°C, but at 37°C neuronal activity is blocked, causing reversible paralysis of the muscles (O'Dowd et al 1989, Pittendrigh et al 1997, Suzuki et al 1971). We previously confirmed that this change in contractility corresponds to a significant change in the contraction magnitude (force generated) in third-instar larvae, of both mutants, relative to wild type, using a mechanical force transducer (Pines et al 2012).

To quantify talin turnover under these different conditions of force, I used FRAP on MTJs of *Drosophila* stage 17 embryos and third-instar larvae. To visualize talin turnover, I used a line

of transgenic flies expressing talin-GFP under control of the promoter from the *ubiquitin* (*ubi*) gene (made by Michael Fairchild). This line both reproduces normal endogenous protein expression and rescues all embryonic defects in *rhea* mutants (Tanentzapf Lab, data not shown). FRAP experiments measure the mobile fraction, the proportion of mobile molecules in the sample region, and the  $t_{1/2}$ , or the speed at which fluorescence recovers to 50% of its maximal value (Reits & Neefjes 2001). The *Drosophila* MTJ is a thin, wide, and linear region, with a high density of integrin-mediated adhesions (thus a high density of IAC components), which makes it easily distinguishable, and ideal for FRAP experiments.

I first tested the effect of increased tensile force on talin turnover by analyzing protein turnover of talin-GFP in *Brkd<sup>J29</sup>* mutant flies. I found that the mobile fraction of talin-GFP at MTJs in *Brkd<sup>J29</sup>* stage 17 embryos is significantly lower at 37°C, compared to embryos at 25°C (Fig. 5a), however the  $t_{1/2}$  of fluorescence recovery does not significantly change (Table 1) indicating that the speed of recovery is the same. The final mobile fraction was reduced from 0.3249 to 0.1229 (Table 1). Talin-GFP in wild type larvae does not exhibit a significant change in mobile fraction, or  $t_{1/2}$  between the two temperatures (Fig. 5c, Table 1).

I subsequently examined the effect of decreased force on talin turnover by performing FRAP on *para<sup>ts2</sup>* mutants expressing talin-GFP (Table 2). Although the *para<sup>ts2</sup>* mutation is well characterized, the temperature sensitive phenotype has only been shown in larvae and adults, thus we used third-instar larvae. In this case, I found that the mobile fraction of talin-GFP at MTJs in *para<sup>ts2</sup>* third-instar larvae is not significantly different at 37°C, compared to larvae at 25°C

**Figure 5 – Force modulates talin turnover at MTJs:** Recovery curves of averaged results from individual FRAP experiments on intact, live stage 17 embryos (a,c) and third-instar larvae (b,d) show that force controls turnover of talin-GFP. Blue indicates 25°C, and red indicates 37°C. (a) To increase tension we used the *Brkd*<sup>J29</sup> allele to cause hypercontraction of the muscles. FRAP results show a highly significant reduction in the mobile fraction of talin-GFP in *Brkd*<sup>J29</sup> mutants after heat-shock at 37°C compared to embryos kept at 25°C (a'). (c) In control embryos (wild type background) there was no significant reduction in the mobile fraction (c'). (b) To decrease tension we used the *para*<sup>ts2</sup> allele to cause paralysis of the muscles. FRAP results reveal that there is no significant change in mobile fraction in larvae kept at 37°C compared to those at 25°C (b'). (d) Larvae expressing talin-GFP in a wild type background show a minor, but significant decrease in mobile fraction (d'). All error bars indicate the standard error of the mean, calculated using a linear regression of our FRAP results.

**Figure 5 – Force modulates talin turnover at MTJs**

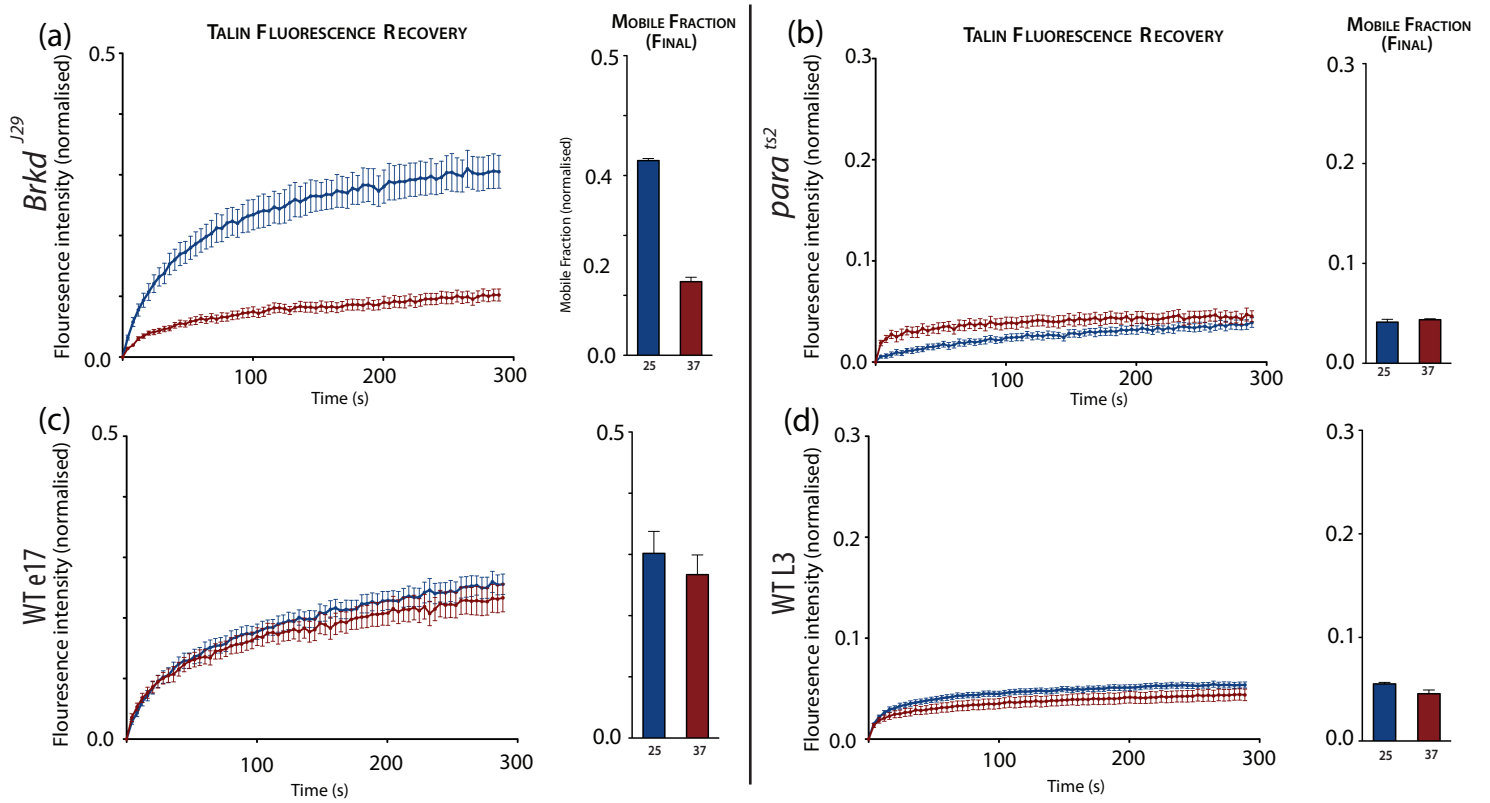


**Table 1 – Mobile fraction and half-time of talin mutants in *Brkd*<sup>J29</sup> mutants**

<b>Genotype (Developmental Stage)</b>	<b>Final MF 25°C (Mean±SEM)</b>	<b>Final MF 37°C (Mean±SEM)</b>
+/talin-GFP (e17)	0.3017±0.03603	0.267±0.03219
<i>Brkd</i> /talin-GFP (e17)	0.3249±0.003519	0.1229±0.0074
<i>Brkd</i> /talin-GFP*R367A (e17)	0.384±0.003966	0.2185±0.00198
<i>Brkd</i> /talin-GFP*KS>DD (e17)	0.2403±0.008669	0.1266±0.003941
<i>Brkd</i> /talin-GFP*Headless (e17)	0.4304±0.01431	0.2922±0.03647
<i>Brkd</i> /talin-GFP*L334R (e17)	0.2317±0.009687	0.1825±0.004435
<i>Brkd</i> /talin-GFP*E1777A (e17)	0.1643±0.003715	0.09803±0.0008912

<b>Genotype (Developmental Stage)</b>	<b>t½ 25°C (95% conf. interval)</b>	<b>t½ 37°C (95% conf. interval)</b>
+/talin-GFP (e17)	48.62 (44.46 to 53.64)	43.4 (38.66 to 49.46)
<i>Brkd</i> /talin-GFP (e17)	39.7 (35.24 to 45.47)	40.56 (35.87 to 46.67)
<i>Brkd</i> /talin-GFP*R367A (e17)	32.43 (30.79 to 34.25)	26.67 (24.55 to 29.17)
<i>Brkd</i> /talin-GFP*KS>DD (e17)	40.33 (36.89 to 44.48)	17.93 (15.01 to 22.26)
<i>Brkd</i> /talin-GFP*Headless (e17)	37.65 (35.81 to 39.69)	25.41 (23.23 to 28.03)
<i>Brkd</i> /talin-GFP*L334R (e17)	37.74 (34.23 to 42.05)	39.45 (37.06 to 42.18)
<i>Brkd</i> /talin-GFP*E1777A (e17)	45.18 (40.62 to 50.91)	25.72 (23.36 to 28.61)

**Table 2 – Mobile fraction and half-time of talin mutants in *para*<sup>ts2</sup> mutants**

<b>Genotype (Developmental Stage)</b>	<b>Final MF 25°C (Mean±SEM)</b>	<b>Final MF 37°C (Mean±SEM)</b>
+/talin-GFP (L3)	0.05513±0.001475	0.04565±0.003613
<i>para</i> /talin-GFP (L3)	0.04411±0.001446	0.04553±0.0004671
<i>para</i> /talin-GFP*R367A (L3)	0.1418±0.002012	0.1987±0.0008551
<i>para</i> /talin-GFP*KS>DD (L3)	0.1336±0.003136	0.1086±0.0005831
<i>para</i> /talin-GFP*Headless (L3)	0.2295±0.02012	0.2757±0.009358
<i>para</i> /talin-GFP*L334R (L3)	0.1086±0.0006994	0.1357±0.0005859
<i>para</i> /talin-GFP*E1777A (L3)	0.08427±0.002473	0.1343±0.002044

<b>Genotype (Developmental Stage)</b>	<b>t½ 25°C (95% conf. interval)</b>	<b>t½ 37°C (95% conf. interval)</b>
+/talin-GFP (L3)	19.28 (17.64 to 21.26)	21.67 (17.96 to 27.32)
<i>para</i> /talin-GFP (L3)	68.55 (57.75 to 84.31)	15.25 (12.37 to 19.89)
<i>para</i> /talin-GFP*R367A (L3)	50.28 (47.33 to 53.63)	13.32 (11.96 to 15.03)
<i>para</i> /talin-GFP*KS>DD (L3)	43.04 (39.07 to 47.90)	20.69 (17.95 to 24.41)
<i>para</i> /talin-GFP*Headless (L3)	43.7 (39.27 to 49.26)	15.95 (14.44 to 17.81)
<i>para</i> /talin-GFP*L334R (L3)	12.66 (11.07 to 14.78)	10.97 (9.169 to 13.66)
<i>para</i> /talin-GFP*E1777A (L3)	20.38 (16.95 to 25.54)	14.6 (12.78 to 17.01)

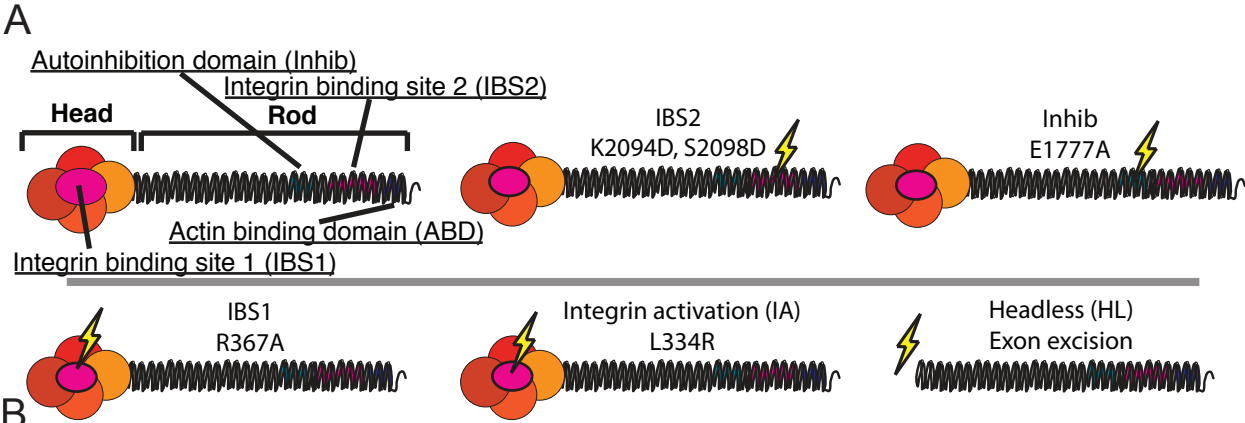
(Fig. 5b,d), but the  $t_{1/2}$  does decrease significantly (Table 2), corresponding to a quicker recovery. Talin-GFP in wild type larvae exposed to the same temperature shift does decrease significantly, but the change is small (Fig. 5d, Table 2), and the  $t_{1/2}$  does not significantly change (Table 2).

### **3.2 Talin turnover regulated in response to increased force does not require integrin binding, auto-inhibition, or the talin FERM domain**

Talin binds to  $\beta$ -integrin tails, activating the integrin heterodimers, and acts as a molecular scaffold for other components of the IAC, and links to the cytoskeleton. These vital and diverse functions are protein-protein interactions, which take place through well-characterized domains within talin. In order to address the question of which domains within talin are required for the appropriate regulation of talin dynamics in response to increased force, I introduced five different GFP-tagged talin mutants into the *Brkd*<sup>J29</sup> background (Fig. 6). These mutations were initially characterized using *in vitro* techniques, CHO cells, and mouse embryonic fibroblasts (Moes et al 2007), and Michael Fairchild made the analogous mutants in *Drosophila* talin. First, I disrupted the FERM domain at varying levels of specificity. One mutation (Headless) removes the entire FERM domain, which contains motifs that bind  $\beta$ -integrin tails, lipids, actin, and other proteins, such as FAK. The second is a point mutation that prevents only binding to  $\beta$ -integrin tails through one integrin-binding site (R367A). This site is required to maintain integrin linkage to the ECM (Ellis et al 2011). The mutation in N-terminal integrin-binding site (IBS1), is analogous to the R358A mutation in vertebrate talin (Garcia-Alvarez et al 2003), and causes lethality and muscle defects (Ellis et al 2011). The third is a different point mutation within IBS1; L334R, or L325R in

**Figure 6 – Schematic of talin mutations used in this thesis:** (a) Illustrations showing the region affected by each mutant used in this thesis, with the relevant amino acid change. (b) Table showing the molecular effect of each mutation.

**Figure 6 – Schematic of talin mutations used in this thesis**



AA-Δ	Molecular effect
E1777A	Disrupts the head-rod interaction that causes autoinhibition
L334R	Disrupts the ability of talin to activate integrins, but does not interfere with binding
R367A	Disrupts a pocket in the FERM domain binds with a Y residue in the β-integrin tail
K2094D, S2098D	Disrupts integrin binding residues in the talin tail

vertebrate talin (Wegener et al 2007). This mutation blocks talin binding to the integrin membrane proximal domain, but does not disrupt talin binding to the membrane distal region of  $\beta$ -integrin tails. The effect of this mutation, in vertebrates, is inhibition of integrin activation by talin. I also disrupted a second integrin-binding site, in the rod region of talin (IBS2), which is important for the linkage of integrin to talin and other IAC components. This mutation of two amino acids, K2094, and S2098 to aspartic acid (KS>DD) is analogous to K2085D, and K2089D in vertebrate talin, and disrupts two key morphogenetic tissue movements during embryogenesis: germ band retraction and dorsal closure (Ellis et al 2011). Lastly, I also prevented autoinhibition of talin using a point mutation (E1777A). Talin and many other FERM domain-containing proteins can fold back on themselves, inhibiting their activity. Structural studies of talin found regions within both the FERM domain and the rod domain that mediate this phenomenon, however we chose to use the mutation in the rod as the corresponding mutation in the head is immediately adjacent to L334 (L325 in vertebrates), which could have unintended effects on integrin binding. A second potential mutation in the head is the subject of controversy in the field (Banno et al 2012, Goksoy et al 2008, Goult et al 2009). The E1777A mutation that we chose is analogous to E1770 in vertebrates, and was shown to completely block autoinhibition (Goult et al 2009). In *Drosophila*, this mutation slows the speed of, and can halt morphogenetic tissue movements (Ellis et al submitted).

I tested the effects of these mutations on force-based control of talin turnover in stage 17 embryos. Surprisingly, I found that all of the tested mutations showed downregulation of turnover in response to increased force (Fig. 7). This effect was less significant in the

**Figure 7 – Reduction of talin turnover via increased force does not require integrin binding, the talin FERM domain, or talin autoinhibition:** Recovery curves of averaged individual FRAP experiments on stage 17 embryos *Brkd*<sup>129</sup> mutants. FRAP assays were conducted to determine the fluorescence recovery (a-f) and mobile fraction (a'-f') of talin-GFP lacking key functional domains. Blue indicates 25°C, and red indicates 37°C. All of tested mutants showed a significant reduction in the mobile fraction after heat-shock at 37°C compared to controls kept at 25°C. Error bars represent standard error.



E1777A mutants (Fig. 7). Notably there is a significant reduction in the  $t_{1/2}$  of turnover in R367A, Headless, KS>DD, and E1777A mutants, compared to no significant change in L334R (Table 1).

### **3.3 Talin turnover regulation in response to reduced force requires binding through IBS1, the FERM domain, and autoinhibition**

To test whether any of these same domains are required for the control of talin turnover in conditions of reduced tensile force using the *para*<sup>ts2</sup> mutation, I introduced the Headless, R367A, L334R, KS>DD, and E1777A mutations into a wild type background, and performed FRAP on the MTJs of third-instar larvae. I then calculated the mobile fraction of talin-GFP, and the  $t_{1/2}$  of fluorescence recovery. I found that integrin binding through IBS1, the FERM domain, and autoinhibition are all required for this control of turnover, as R367A, Headless, L334R, and E1777A exhibit an increase in turnover in response to reduced force (Fig. 8). The KS>DD mutant shows a slight but significant reduction in turnover (Fig. 8). The  $t_{1/2}$  exhibits a highly significant reduction in turnover in all cases (Table 2).

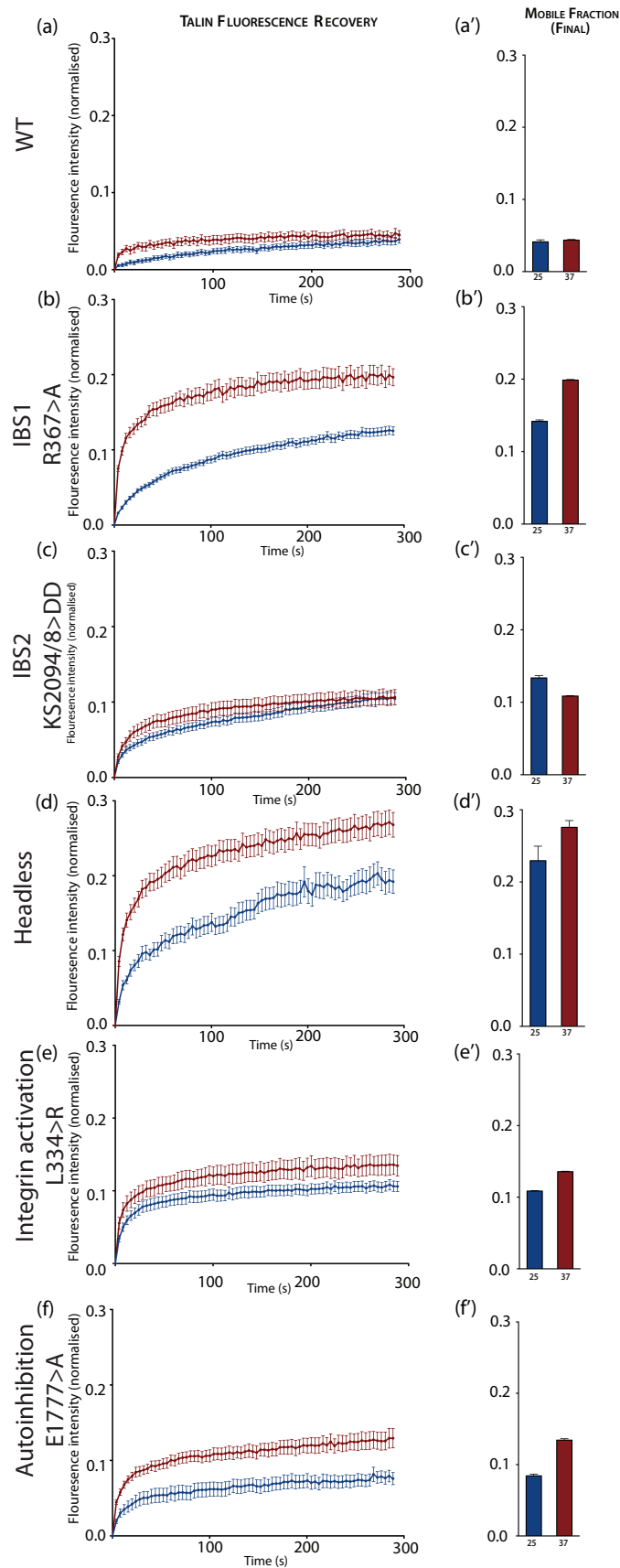
### **3.4 Regulation of talin turnover at the onset of muscle contractility requires physical binding to $\beta$ -integrin tails, but not activation**

In addition to using conditional mutants to modulate tensile force, I also examined the dynamics of talin during a normal developmental process in which force increases by a great magnitude: embryonic and larval muscle development. Integrin-mediated adhesion is vital for a number of dynamic morphogenetic processes during *Drosophila* embryogenesis. One of these processes is muscle development. Talin is required for fully adherent muscles, and talin

**Figure 8 – Control of talin turnover in response to reduced force requires integrin binding through IBS1, the FERM domain, and autoinhibition:**

Recovery curves of averaged individual FRAP experiments on third-instar *para*<sup>ts2</sup> larvae. FRAP assays were conducted to determine the fluorescence recovery (a-f) and mobile fraction (a'-f') of talin-GFP lacking key functional domains. Blue indicates 25°C, and red indicates 37°C. R367A, Headless, L334R, and E1777A all exhibit a significant increase in mobile fraction upon reduction of force, whereas KS>DD exhibits a slight, but significant reduction in mobile fraction compared to the corresponding 25°C controls. Error bars represent standard error.

**Figure 8 – Control of talin turnover in response to reduced force requires integrin binding through IBS1, the FERM domain, and autoinhibition**



null mutants phenocopy integrin null (*mys*) mutants (Brown et al 2002). Muscles of the *Drosophila* embryo are fully formed, but quiescent by stage 16. The first change in force is the onset of muscle contraction, which occurs at stage 17, the final stage of embryogenesis (Broadie & Bate 1993). After the larvae hatch and begin to grow, the musculature greatly increases in size. MTJ width grows by a factor of four, volume increases by a factor of fifteen (Yuan et al 2010), and locomotion speed also increases during this time. This equates to a large increase in tensile force on MTJs. Unsurprisingly, our lab showed that turnover of integrin and IAC components decrease in successive steps during development (Yuan et al 2010). I introduced the Headless, R367A, L334R, KS>DD, and E1777A mutations into a wild type background and performed FRAP during 5 distinct developmental stages (stage 16 and 17 embryos, and first-, second-, and third-instar larvae) (Fig. 9, Table 3). All of the tested mutations showed the appropriate downregulation of turnover between embryonic and larval stages, however the Headless, and R367A mutations do not exhibit the wildtype pattern of downregulation of turnover from stage 16 to stage 17 of embryogenesis (Fig. 9). The L334R mutation, on the other hand, does not have a similar effect to Headless or R367A, indicating that physical binding of talin to integrin is required for this control of dynamics, but the conformational change that talin causes in integrin, in vertebrate cells, is not required. This result is at odds with the previous results of experiments using *Brkd*<sup>J29</sup>, and potential reasons for this will be discussed in the following chapter.

**Figure 9 – Downregulation of talin turnover at the onset of muscle activity requires binding through IBS1:** Averaged recovery curves of FRAP experiments on stage 16, 17, embryos, and first-, second-, and third-instar larvae (a-f), and corresponding mobile fractions (a'-f') of talin-GFP with mutations in key functional domains. Recovery decreases significantly between embryonic and larval stages in all cases, however talin-GFP mutants that cannot bind to  $\beta$ -integrin tails (Headless, R367A) do not exhibit downregulated turnover between embryonic stage 16 and 17. Error bars represent standard error.

**Figure 9 – Downregulation of turnover at the onset of muscle activity requires binding through IBS1**

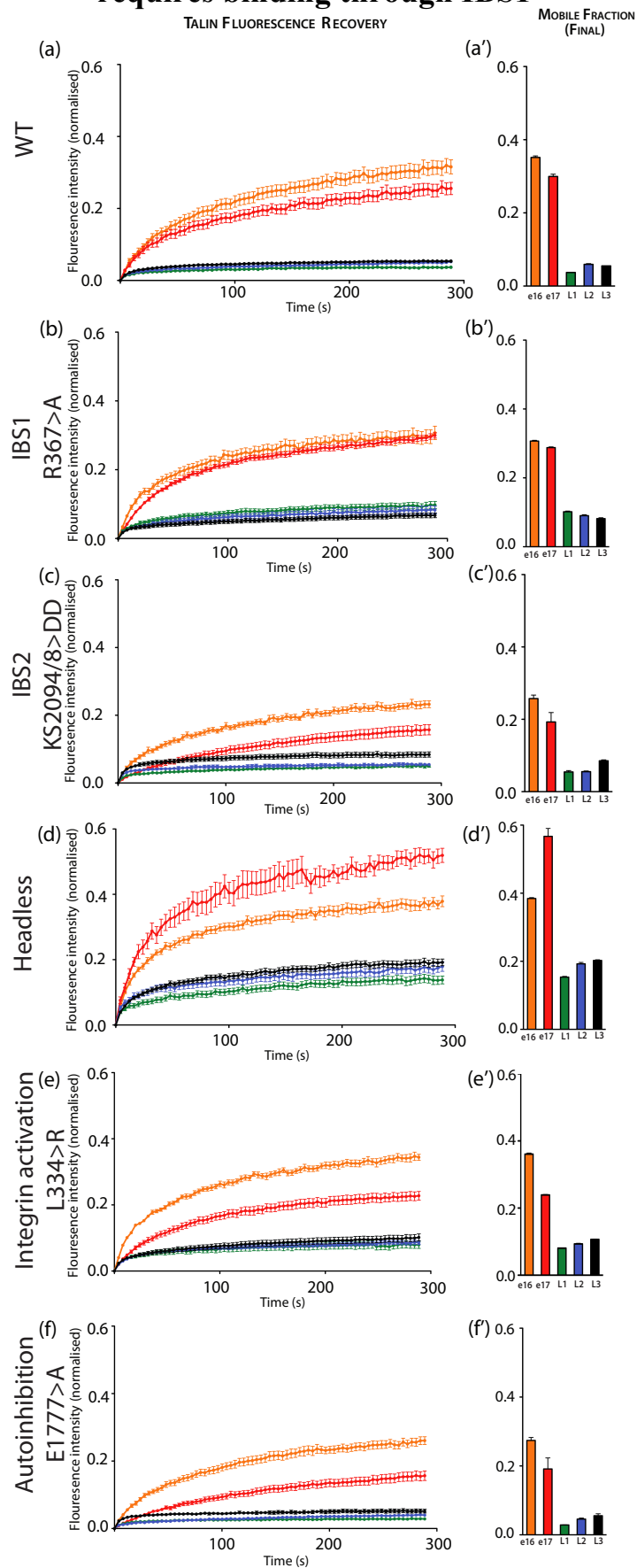


**Table 3 – Mobile fraction and half-time of talin mutants during development**

<b>Genotype (Developmental Stage)</b>	<b>Final MF (Mean±SEM)</b>	<b>t½ (95% conf. interval)</b>
+/talin-GFP (e16)	0.3516±0.004129	52 (47.98 to 56.76)
+/talin-GFP (e17)	0.2995±0.006242	48.62 (44.46 to 53.64)
+/talin-GFP (L1)	0.03711±0.0002817	18.73 (16.47 to 21.72)
+/talin-GFP (L2)	0.05934±0.00205	25.5 (23.51 to 27.86)
+/talin-GFP (L3)	0.05508±0.0003123	19.28 (17.64 to 21.26)
+/talin-GFP*R367A (e16)	0.3069±0.002167	34.28 (32.22 to 36.61)
+/talin-GFP*R367A (e17)	~ 0.4152±~ 0.04558	44.59 (42.45 to 46.95)
+/talin-GFP*R367A (L1)	0.1017±0.001105	31.63 (28.67 to 35.26)
+/talin-GFP*R367A (L2)	0.09012±0.001628	34.1 (30.79 to 38.21)
+/talin-GFP*R367A (L3)	0.08179±0.001781	30.74 (26.99 to 35.70)
+/talin-GFP*KS>DD (e16)	0.2574±0.009575	48.98 (46.19 to 52.12)
+/talin-GFP*KS>DD (e17)	0.1928±0.02583	79.85 (69.49 to 93.84)
+/talin-GFP*KS>DD (L1)	0.05444±0.003904	25.01 (22.11 to 28.79)
+/talin-GFP*KS>DD (L2)	0.05528±0.002038	9.816 (8.181 to 12.27)
+/talin-GFP*KS>DD (L3)	0.08525±0.002667	14.7 (12.69 to 17.46)
+/talin-GFP*Headless (e16)	0.362±0.002668	29.27 (27.22 to 31.65)
+/talin-GFP*Headless (e17)	0.4939±0.004187	31.14 (28.93 to 33.71)
+/talin-GFP*Headless (L1)	0.1433±0.002491	35.2 (31.31 to 40.20)
+/talin-GFP*Headless (L2)	0.1691±0.002547	24 (21.10 to 27.83)
+/talin-GFP*Headless (L3)	0.1874±0.00193	29.7 (27.04 to 32.94)
+/talin-GFP*L334R (e16)	0.3608±0.002742	38.81 (36.24 to 41.79)
+/talin-GFP*L334R (e17)	0.2392±0.001232	48.26 (46.21 to 50.51)
+/talin-GFP*L334R (L1)	0.08073±0.0007164	19.85 (17.70 to 22.58)
+/talin-GFP*L334R (L2)	0.09325±0.001492	22.6 (20.30 to 25.47)
+/talin-GFP*L334R (L3)	0.1065±0.0007638	31.8 (28.61 to 35.78)
+/talin-GFP*E1777A (e16)	0.2741±0.008558	51.36 (48.05 to 55.17)
+/talin-GFP*E1777A (e17)	0.1914±0.03184	80.41 (71.50 to 91.85)
+/talin-GFP*E1777A (L1)	0.02868±0.0008661	11.82 (10.12 to 14.22)
+/talin-GFP*E1777A (L2)	0.04567±0.002995	41.2 (37.66 to 45.46)
+/talin-GFP*E1777A (L3)	0.05549±0.005511	8.977 (7.334 to 11.57)

### 3.5 High temporal resolution quantification of talin turnover

#### 3.5.1 *Increased tensile force reduces talin recycling*

In previous work we quantified the turnover of integrin, tensin, and ILK under conditions of altered tensile force. We quantified the mobile fraction, but also modeled the recovery curves using ordinary differential equations to further describe the recovery kinetics, allowing us to better understand the mechanism by which tensile force modulates protein turnover at adhesive sites. To briefly summarize, we found that increased force reduces integrin turnover by slowing the rate of integrin endocytosis from the membrane, and requires previously described mechanosensing and signaling domains. Reduced force causes increased integrin endo and exocytosis, but overall levels of integrin are stabilized, again via mechanosensing and signaling. For the members of the adhesion complex, we found an inverse relationship between tensile force and overall mobile fraction. The mathematical model for turnover of those proteins is more elaborate, and must account for both endocytic recycling and binding interactions with the complex, for a total of four parameters (as opposed to two for integrin). However, fitting the curves to that model was uninformative as our FRAP technique quantified recovery too infrequently.

To expand on our previous work, and to allow us to better understand how force controls adhesion stability on a mechanistic level, I modified our FRAP protocol. Under this new protocol I collected new datasets for GFP-tagged tensin and ILK, using *Brkd*<sup>J29</sup> and *para*<sup>ts2</sup> to modulate force, and expanded the analysis to include GFP-tagged talin. We then fit the recovery curves to the four-parameter model of recovery. These four parameters take into

account binding on ( $k_{on}$ ) and binding off ( $k_{off}$ ) of the protein to integrin or the IAC, and endocytosis ( $k_{endo}$ ) and exocytosis ( $k_{exo}$ ) to and from the membrane.

I first examined the recovery of GFP-tagged talin under increased tensile force using the *Brkd*<sup>J29</sup> mutation in stage 17 embryos. Talin is a vital component of integrin adhesion in all model systems, and is conformationally changed by tensile force, making it an ideal starting point for this detailed analysis. The results of fitting the recovery curves to our model showed that, relative to wild type, talin under increased force showed significantly reduced values for  $k_{on}$  and  $k_{off}$ , and a significantly reduced  $k_{endo}$ , while the  $k_{exo}$  does not change (Fig. 10a-d, Table 4). To understand the overall effect that these shifts have on the level of binding and recycling of talin, I calculated  $K_{bind}$  ( $k_{on}/k_{off}$ ), and  $K_{recycling}$  ( $k_{endo}/k_{exo}$ ). If  $K_{bind}$  increases, it is indicative of an overall increase in bound protein. If  $K_{recycling}$  increases, it is indicative of an increase in internalization of protein, meaning less availability for binding at the MTJ. For talin, increased force does not significantly change  $K_{bind}$ , but  $K_{recycling}$  is significantly decreased (Table 4). The result indicates that force stabilizes talin already in the IAC by reducing binding and unbinding, and slows endocytic recycling, increasing availability at the membrane.

**Figure 10 – Characterization of the effect of force on talin dynamics:**

Calculated parameter values for binding on, binding off, endocytosis, and exocytosis of talin-GFP in wildtype and *Brkd*<sup>J29</sup> mutants in stage 17 embryos (a-d) and in wildtype and *para*<sup>ts2</sup> mutants in 3<sup>rd</sup> instar larvae (a'-d'). Error bars indicate standard deviation and orange arrows indicate the directionality of a significant change in the parameter value.

**Figure 10 – Characterization of the effect of force on talin dynamics**

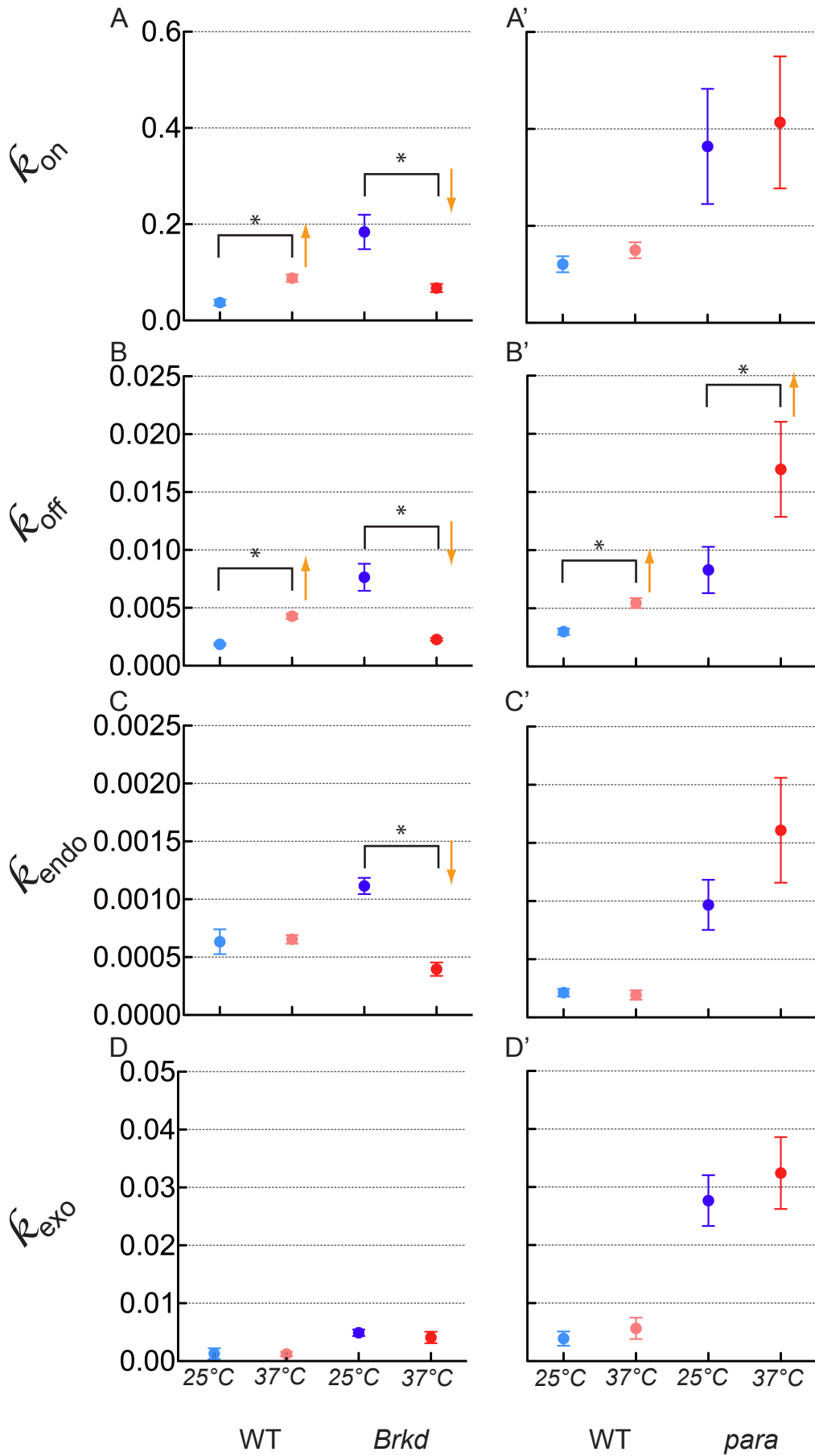


**Table 4 – Rate constants of talin turnover under increased force**

	<b>Parameter</b>	<b>Best fit estimate</b>	<b>Standard deviation</b>
<b>e17 talin WT 25°C</b>	kon	0.037105024	0.006159998
	koff	0.001847205	9.74E-05
	kendo	0.000633552	0.000107451
	kexo	0.001296521	0.000918558
	K_bind	20.08711773	3.499088156
	K_recycle	0.488655197	0.355983638
	f_max	0.349990201	
<b>e17 talin WT 37°C</b>	kon	0.087844399	0.007801771
	koff	0.004269319	0.000229295
	kendo	0.000653602	3.75E-05
	kexo	0.001224963	0.000382488
	K_bind	20.57573972	2.135554916
	K_recycle	0.533568731	0.169396305
	f_max	0.36795653	
<b>e17 talin <i>Brkd</i> 25°C</b>	kon	0.183954373	0.035826668
	koff	0.00763468	0.001166024
	kendo	0.001114855	7.00E-05
	kexo	0.004893716	0.000564547
	K_bind	24.09457584	5.963419229
	K_recycle	0.227813569	0.029924843
	f_max	0.212174542	
<b>e17 talin <i>Brkd</i> 37°C</b>	kon	0.067361735	0.008729952
	koff	0.002265399	0.000128041
	kendo	0.000396012	5.77E-05
	kexo	0.00408143	0.000988863
	K_bind	29.73503928	4.204140156
	K_recycle	0.097027739	0.027427739
	f_max	0.115559333	

### 3.5.2 *Decreased tensile force does not change overall rates of talin binding or recycling*

Subsequently, I used the *para*<sup>ts2</sup> mutation to reduce tensile force on the IAC and performed FRAP on GFP-tagged third-instar larvae. After fitting the results to our model, we found that neither  $k_{on}$  nor  $k_{off}$  significantly changed relative to the control genotype ( $k_{off}$  does significantly increase, but this effect is the same with the control) (Fig. 10a'-b', Table 5).  $K_{endo}$  and  $k_{exo}$  do not significantly change with reduced force, nor in the controls (Fig. 10c'-d', Table 5). There is a significant decrease in the overall binding, as indicated by  $K_{bind}$ , but this effect is seen in the controls as well. The value of  $K_{recycling}$  does not significantly change (Table 5).

**Table 5 – Rate constants of talin turnover under reduced force**

	<b>Parameter</b>	<b>Best fit estimate</b>	<b>Standard deviation</b>
<b>L3 talin WT 25°C</b>	kon	0.12081794	0.016517391
	koff	0.002998405	0.000274769
	kendo	0.00021257	3.28E-05
	kexo	0.00388997	0.001224394
	K_bind	40.29407344	6.631780005
	K_recycle	0.054645544	0.019155663
	f_max	0.073613531	
<b>L3 talin WT 37°C</b>	kon	0.149803696	0.01647649
	koff	0.005450976	0.000431323
	kendo	0.000192318	4.04E-05
	kexo	0.005648462	0.001842548
	K_bind	27.48199615	3.723620146
	K_recycle	0.034047893	0.013210297
	f_max	0.065800659	
<b>L3 talin <i>para</i> 25°C</b>	kon	0.363821981	0.118797393
	koff	0.008297173	0.001992239
	kendo	0.00096747	0.000215273
	kexo	0.027662487	0.004375535
	K_bind	43.84890818	17.77219666
	K_recycle	0.034974066	0.009548041
	f_max	0.054623523	
<b>L3 talin <i>para</i> 37°C</b>	kon	0.413573648	0.136205217
	koff	0.016948927	0.004086612
	kendo	0.001608667	0.000450695
	kexo	0.032412357	0.006188131
	K_bind	24.4011695	9.959703368
	K_recycle	0.049631289	0.016826648
	f_max	0.083084409	

### 3.6 High temporal resolution quantification of tensin turnover

#### 3.6.1 *Increased tensile force increases tensin exocytosis*

I then used the modified FRAP protocol to quantify turnover of GFP-tagged tensin under control of the endogenous promoter, and in conditions of high force using the *Brkd*<sup>J29</sup> mutation in stage 17 embryos. Tensin is a key component of the IAC, and especially relevant to understanding how mechanical force modulates dynamics, due to its actin capping, aggregating, and crosslinking ability. In order to effectively transduce force, there must be connection to the cytoskeleton. After fitting the data to our model, we found that under high force,  $k_{on}$  increased significantly, as did  $k_{off}$ . Although the relative increase in  $k_{on}$  was larger,  $K_{bind}$  increased nonsignificantly (Fig. 11a-b, Table 6), indicating that the balance of bound versus unbound tensin was stable. The control force condition saw a significant decrease in  $k_{on}$ , and  $k_{off}$ , and a nonsignificant decrease in  $K_{bind}$  (Fig. 11a-b, Table 6). The  $k_{endo}$  of tensin significantly decreased, compared to the control, and  $k_{exo}$  did not significantly increase compared to the control (Fig. 11c-d). This reduction of  $k_{endo}$  leads to an overall decrease in  $K_{recycling}$ , meaning that more tensin is available at the membrane (Table 6). The controls showed no significant change in either  $K_{bind}$  or  $K_{recycling}$  (Table 6).

#### 3.6.2 *Decreased tensile force decreases overall tensin binding, and increases exocytosis*

Under conditions of reduced force, using the *para*<sup>ts2</sup> mutation, I performed FRAP on GFP-tagged tensin in third-instar larvae, and we then fitted the results to our model. The results show statistically significant increases in both  $k_{on}$  and  $k_{off}$  of tensin, whereas our control

**Figure 11 – Characterization of the effect of force on tensin dynamics:**

Calculated parameter values for binding on, binding off, endocytosis, and exocytosis of tensin::GFP in wildtype and *Brkd*<sup>129</sup> mutants in stage 17 embryos (a-d) and in wildtype and *para*<sup>ts2</sup> mutants in 3<sup>rd</sup> instar larvae (a'-d'). Error bars indicate standard deviation and orange arrows indicate the directionality of a significant change in the parameter value.

**Figure 11 – Characterization of the effect of force on tensin dynamics**

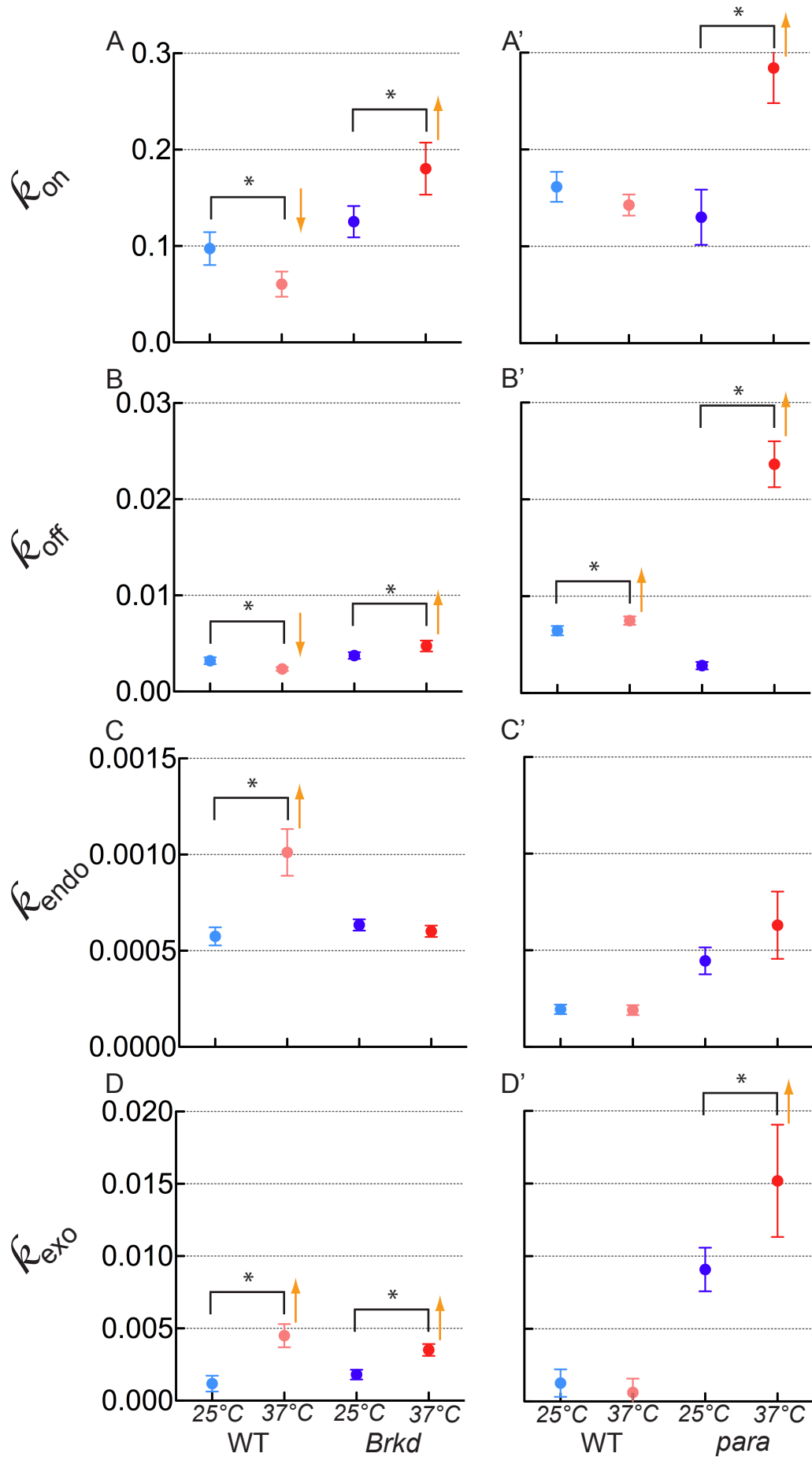


**Table 6 – Rate constants of tensin turnover under increased force**

	<b>Parameter</b>	<b>Best fit estimate</b>	<b>Standard deviation</b>
<b>e17 tensin WT 25°C</b>	kon	0.097311486	0.017017805
	koff	0.00319884	0.000357585
	kendo	0.000574725	4.70E-05
	kexo	0.001177611	0.000548053
	K_bind	30.42086629	6.313996261
	K_recycle	0.488043278	0.230612342
	f_max	0.342501255	
<b>e17 tensin WT 37°C</b>	kon	0.060351375	0.013049794
	koff	0.002341513	0.000195698
	kendo	0.001011187	0.000121351
	kexo	0.004493466	0.000800629
	K_bind	25.77452014	5.975061945
	K_recycle	0.225034958	0.048342624
	f_max	0.208756198	
<b>e17 tensin Brkd 25°C</b>	kon	0.12521948	0.016232256
	koff	0.003739821	0.00034767
	kendo	0.00063409	2.94E-05
	kexo	0.001800368	0.000338013
	K_bind	33.48274941	5.341147643
	K_recycle	0.352200334	0.068113038
	f_max	0.276445794	
<b>e17 tensin Brkd 37°C</b>	kon	0.180231956	0.027015716
	koff	0.004730875	0.000562201
	kendo	0.000601281	2.96E-05
	kexo	0.003506944	0.000410562
	K_bind	38.09696376	7.287421582
	K_recycle	0.171454325	0.021774753
	f_max	0.165068563	

genotype showed a significant increase only in  $k_{\text{off}}$  (Fig. 11a'-b'). We also found a significant increase in  $k_{\text{exo}}$ , but not  $k_{\text{endo}}$  (Fig 11c'-d'). The magnitude of shift in the binding and unbinding coefficients was such that there is a significant decrease in the amount of bound tensin, as indicated by  $K_{\text{bind}}$ , but no significant change in overall recycling, as indicated by  $K_{\text{recycling}}$  (Table 7).

**Table 7 – Rate constants of tensin turnover under reduced force**

	<b>Parameter</b>	<b>Best fit estimate</b>	<b>Standard deviation</b>
<b>L3 tensin WT 25°C</b>	kon	0.161446898	0.015541256
	koff	0.006436932	0.000486284
	kendo	0.00019423	2.47E-05
	kexo	0.001264118	0.000945938
	K_bind	25.08134082	3.069122441
	K_recycle	0.153648666	0.11662356
	f_max	0.162141493	
<b>L3 tensin WT 37°C</b>	kon	0.142672267	0.010890495
	koff	0.007478983	0.000435386
	kendo	0.000190345	2.56E-05
	kexo	0.000617638	0.00095523
	K_bind	19.07642722	1.831291998
	K_recycle	0.308182534	0.478432258
	f_max	0.26503189	
<b>L3 tensin <i>para</i> 25°C</b>	kon	0.130050216	0.028456301
	koff	0.002832208	0.000387729
	kendo	0.000445269	6.95E-05
	kexo	0.009083115	0.001500909
	K_bind	45.91831861	11.85185946
	K_recycle	0.049021619	0.011142848
	f_max	0.066118284	
<b>L3 tensin <i>para</i> 37°C</b>	kon	0.284105291	0.03625079
	koff	0.02362603	0.002369428
	kendo	0.000629811	0.000174031
	kexo	0.015186232	0.003865219
	K_bind	12.02509665	1.9515765
	K_recycle	0.041472531	0.015580382
	f_max	0.110820208	

### 3.7 High temporal resolution quantification of ILK turnover

#### 3.7.1 *Increased tensile force increases overall ILK binding*

ILK is an important scaffold in the IAC, allowing correct localization of other focal adhesion proteins, and mediating signaling events that occur through integrin adhesions. I visualized ILK turnover at the MTJ using GFP-tagged ILK under control of the endogenous promoter in both embryonic stage 17 and third-instar larvae, in conditions of high and low tensile force, respectively. I then quantified this turnover using FRAP, and fitted the data to our model. When increasing force using the *Brkd*<sup>J29</sup> mutation, the resulting parameter values showed an increase in both  $k_{on}$  and  $k_{off}$ , and  $k_{endo}$  and  $k_{exo}$  (Fig. 12a-d). However, calculating the  $K_{bind}$  and  $K_{recycling}$  shows a significant increase in  $K_{bind}$ , and no change in  $K_{recycling}$  (Table 8). The control condition, in which force was not modified, showed no change in  $k_{on}$  and  $k_{off}$ , and significant reductions of  $k_{endo}$  and  $k_{exo}$  (Fig. 12a-d). The magnitude of these changes results no significant change in  $K_{bind}$  or  $K_{recycling}$  (Table 8).

#### 3.7.2 *Decreased force decreases ILK binding*

Finally, I decreased force at the MTJ using the *para*<sup>ts2</sup> mutation, and imaged GFP-tagged ILK recovery with FRAP. Then we modeled the recovery curves and the resulting numerical parameters show a significant increase in  $k_{on}$  and  $k_{off}$ , and a significant increase in  $k_{exo}$  and  $k_{endo}$  (Fig. 12a'-d', Table 9). Then, by calculating  $K_{bind}$ , we find a significant decrease (Table 9), indicating a reduction in bound ILK. The change in  $K_{recycling}$  after force reduction is non-significant (Table 9). Our force control genotype also showed a decrease in  $K_{bind}$ , but this is due to a decrease in  $k_{on}$ , rather than increasing  $k_{off}$  (Table 9).

**Figure 12 – Characterization of the effect of force on ILK dynamics:**

Calculated parameter values for binding on, binding off, endocytosis, and exocytosis of ILK::GFP in wildtype and *Brkd*<sup>129</sup> mutants in stage 17 embryos (a-d) and in wildtype and *para*<sup>ts2</sup> mutants in 3<sup>rd</sup> instar larvae (a'-d'). Error bars indicate standard deviation and orange arrows indicate the directionality of a significant change in the parameter value.

**Figure 12 – Characterization of the effect of force on ILK dynamics**

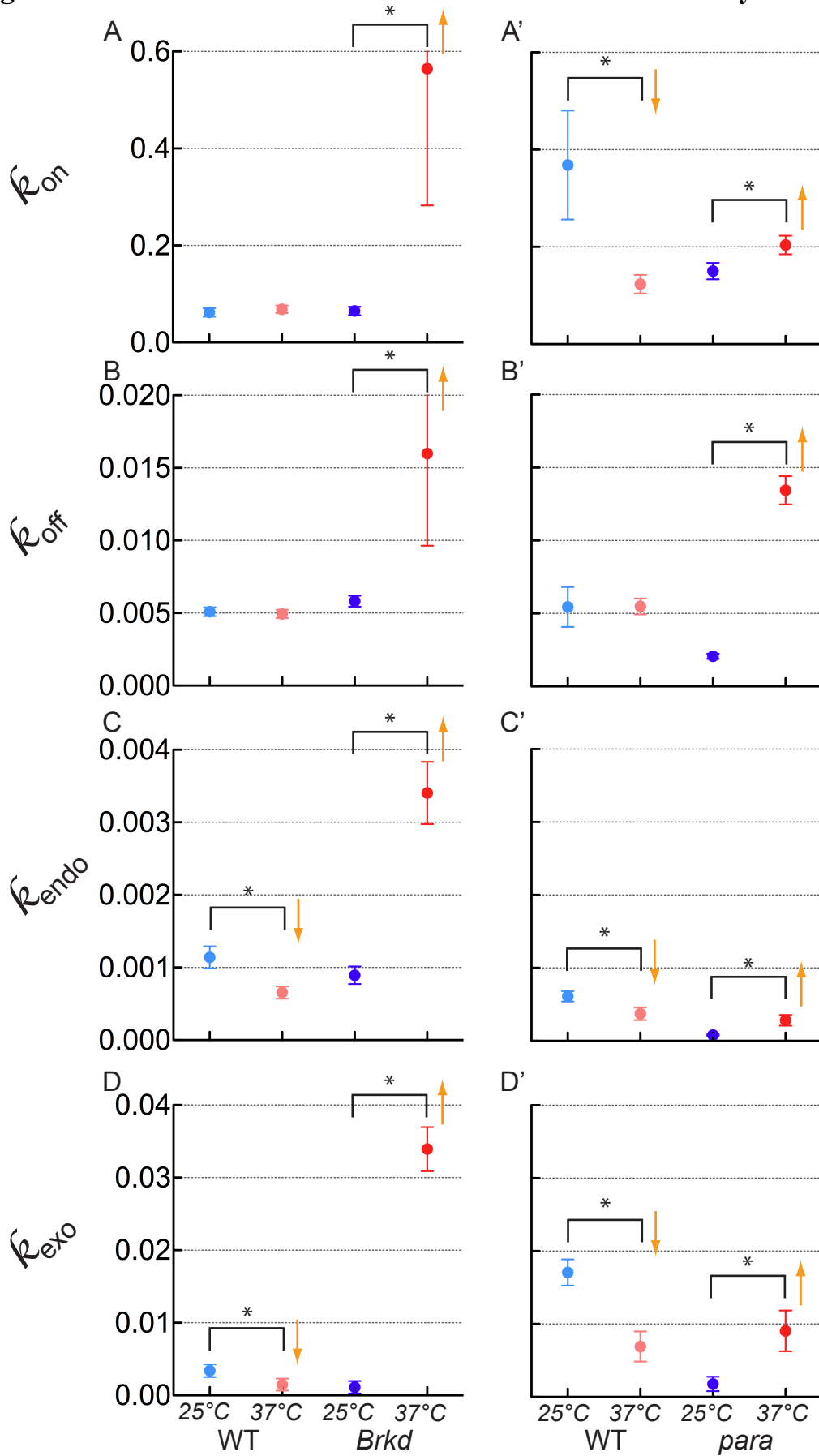


**Table 8 – Rate constants of ILK turnover under increased force**

	<b>Parameter</b>	<b>Best fit estimate</b>	<b>Standard deviation</b>
<b>e17 ILK WT 25°C</b>	kon	0.061906943	0.00884394
	koff	0.005087699	0.000302595
	kendo	0.001138943	0.000152267
	kexo	0.003388045	0.000877136
	K_bind	12.16796387	1.882929433
	K_recycle	0.336165154	0.097949351
	f_max	0.294954497	
<b>e17 ILK WT 37°C</b>	kon	0.0683612	0.007921067
	koff	0.004938969	0.000287075
	kendo	0.000654938	8.50E-05
	kexo	0.001474847	0.000825985
	K_bind	13.84118917	1.794263303
	K_recycle	0.444071632	0.255291944
	f_max	0.340508495	
<b>e17 ILK <i>Brkd</i> 25°C</b>	kon	0.06485029	0.008626967
	koff	0.005814399	0.000377145
	kendo	0.000893306	0.000121199
	kexo	0.001115258	0.000850523
	K_bind	11.15339463	1.650703544
	K_recycle	0.800985687	0.620443084
	f_max	0.471079833	
<b>e17 ILK <i>Brkd</i> 37°C</b>	kon	0.564319962	0.281722531
	koff	0.015983002	0.006343676
	kendo	0.003403912	0.000428473
	kexo	0.033923849	0.003032367
	K_bind	35.30750773	22.51822339
	K_recycle	0.100339803	0.015491054
	f_max	0.113995463	

**Table 9 – Rate constants of ILK turnover under reduced force**

	<b>Parameter</b>	<b>Best fit estimate</b>	<b>Standard deviation</b>
<b>L3 ILK WT 25°C</b>	kon	0.368341386	0.111964428
	koff	0.005443735	0.001363932
	kendo	0.000610407	7.15E-05
	kexo	0.017064017	0.001790059
	K_bind	67.66335391	26.65394637
	K_recycle	0.035771568	0.005624806
	f_max	0.048118211	
<b>L3 ILK WT 37°C</b>	kon	0.123226926	0.019135495
	koff	0.005481109	0.000542313
	kendo	0.000371284	8.69E-05
	kexo	0.006915248	0.002062756
	K_bind	22.48211508	4.139609988
	K_recycle	0.053690638	0.020357047
	f_max	0.089394538	
<b>L3 ILK <i>para</i> 25°C</b>	kon	0.150155532	0.016787027
	koff	0.002061318	0.000175869
	kendo	8.00E-05	1.06E-05
	kexo	0.001785233	0.000986049
	K_bind	72.84443503	10.24442085
	K_recycle	0.044836994	0.025466946
	f_max	0.055324789	
<b>L3 ILK <i>para</i> 37°C</b>	kon	0.203749897	0.019103589
	koff	0.013443918	0.000968241
	kendo	0.00028202	7.34E-05
	kexo	0.009051531	0.002790989
	K_bind	15.15554455	1.791813854
	K_recycle	0.031157149	0.012568627
	f_max	0.088538962	

### **3.8 High temporal resolution quantification of turnover throughout development**

Our lab previously observed a downregulation of IAC protein turnover during developmental progression from late embryogenesis to the end of larval development. The data collected for the previous analysis on the mechanisms behind regulation of IAC turnover in response to force allowed us to investigate the role of force in the developmental regulation of protein turnover. Examining the changes in rate constants between stage 17 embryos and third-instar larvae showed a significant increase in  $k_{on}$  in talin, tensin and ILK, however this is balanced out by an increase in  $k_{off}$  for talin and tensin, but not ILK (Fig. 13a-a'', b-b''). All proteins show a significant decrease in the rate of endocytosis (Fig. 13c-c''), and this reduction of overall recycling is further exacerbated by increases in the exocytosis of talin and ILK, but not tensin (Fig. 13d-d'')(Table 10). The result for talin and tensin indicate that changes in mobility during development are dominated by control of recycling alone, whereas the results for ILK indicate a role for increased binding to the complex, in addition to recycling.

**Figure 13 – Talin and ILK are downregulated during development in a manner distinct from force alone:** Calculated values for (a-a'')  $k_{on}$ , (b-b'')  $k_{off}$ , (c-c'')  $k_{endo}$ , and (d-d'')  $k_{exo}$  in stage 17 embryos (red) and 3<sup>rd</sup> instar larvae (black) expressing GFP-tagged talin (a-d), tensin (a'-d'), or ILK (a''-d''). Results show an increase in  $k_{on}$  in all 3 proteins, and an increase in  $k_{off}$  with talin and tensin during progression from stage 17 embryos to 3<sup>rd</sup> instar larvae. During the same period,  $k_{endo}$  is decreased across all proteins, and  $k_{exo}$  increases in talin and ILK. Asterisks indicate significance, and the arrows show the directionality of change.

**Figure 13 – Characterization of turnover regulation during development**

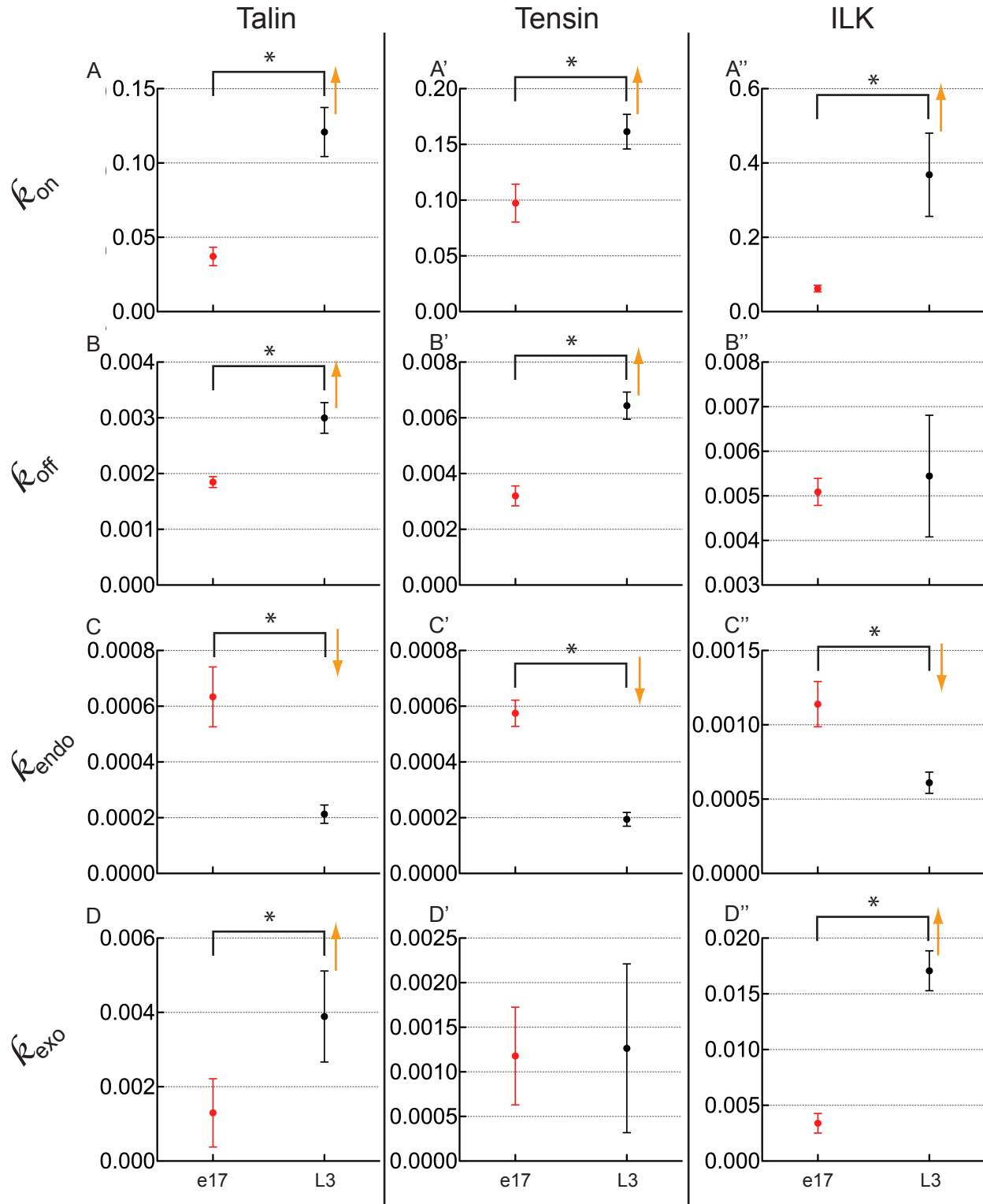


**Table 10 – Rate constants of talin, tensin, and ILK in stage 17 embryos and 3<sup>rd</sup> instar larvae**

	<b>Parameter</b>	<b>Best fit estimate</b>	<b>Standard deviation</b>
<b>e17 talin WT</b>	kon	0.037105024	0.006159998
	koff	0.001847205	9.74E-05
	kendo	0.000633552	0.000107451
	kexo	0.001296521	0.000918558
	K_bind	20.08711773	3.499088156
	K_recycle	0.488655197	0.355983638
	f_max	0.349990201	
<b>L3 talin WT</b>	kon	0.12081794	0.016517391
	koff	0.002998405	0.000274769
	kendo	0.00021257	3.28E-05
	kexo	0.00388997	0.001224394
	K_bind	40.29407344	6.631780005
	K_recycle	0.054645544	0.019155663
	f_max	0.073613531	
<b>e17 tensin WT</b>	kon	0.097311486	0.017017805
	koff	0.00319884	0.000357585
	kendo	0.000574725	4.70E-05
	kexo	0.001177611	0.000548053
	K_bind	30.42086629	6.313996261
	K_recycle	0.488043278	0.230612342
	f_max	0.342501255	
<b>L3 tensin WT</b>	kon	0.161446898	0.015541256
	koff	0.006436932	0.000486284
	kendo	0.00019423	2.47E-05
	kexo	0.001264118	0.000945938
	K_bind	25.08134082	3.069122441
	K_recycle	0.153648666	0.11662356
	f_max	0.162141493	
<b>e17 ILK WT</b>	kon	0.061906943	0.00884394
	koff	0.005087699	0.000302595
	kendo	0.001138943	0.000152267
	kexo	0.003388045	0.000877136
	K_bind	12.16796387	1.882929433
	K_recycle	0.336165154	0.097949351
	f_max	0.294954497	
<b>L3 ILK WT</b>	kon	0.368341386	0.111964428
	koff	0.005443735	0.001363932
	kendo	0.000610407	7.15E-05
	kexo	0.017064017	0.001790059
	K_bind	67.66335391	26.65394637
	K_recycle	0.035771568	0.005624806
	f_max	0.048118211	

## **Chapter 4: Discussion and Conclusion**

### **4.1 Force regulates talin turnover**

The experiments presented in this thesis are the first study on mechano-regulation of talin dynamics in live animals. The MTJs, used as a model for long-term cell-ECM adhesion, form during late embryogenesis and must remain attached throughout the remodeling and size increases that occur during the five-day larval development (Volk & VijayRaghavan 1994, Wright 1960). The overall conclusion from this work is that force increases the stability of adhesions, while lack of force increases the plasticity of adhesions. Although the experiments did not uncover any domains required for the control of talin turnover in response to increased force, the results do rule out many key domains, and provide evidence of strong redundancy in the system. We also uncover three talin domains that are necessary for the appropriate control of talin turnover in response to decreased tensile force, and demonstrate one talin domain that is important for control of turnover at the onset of muscle contractility during normal development. Finally, novel methodology used for these experiments, combined with advanced mathematical modeling, allows us to highlight the unique ways in which each protein, talin, tensin and ILK, respond to force.

Our lab recently showed that adhesion turnover is regulated in a force-dependent manner, and that both integrins themselves, and the components of the intra-cellular adhesion complex tensin and ILK, are stabilized or destabilized based on the level of force transmitted through adhesions (Pines et al 2012). Talin is an incredibly important part of integrin-mediated adhesion, functioning as a structural and signaling hub, and was one of the first

proteins shown to be conformationally changed by a physiologically relevant level of force (del Rio et al 2009). As a part of the IAC, it was expected to respond to force in a manner similar to tensin and ILK, with high force reducing turnover, and low force increasing turnover. However, the results showed that although increasing force reduces turnover, decreasing force does not change the percentage of mobile talin; instead the speed of turnover in that mobile population is increased. This effect mirrors the response of integrin to tensile force (Pines et al 2012). The results are also consistent with research showing that force can regulate adhesion complex assembly and function in cell culture. In that system, high force leads to adhesion assembly and maturation, and low force leads to more dynamic focal adhesions, and disassembly in nascent adhesions, but not in some populations of mature adhesions (Balaban et al 2001, Pelham & Wang 1997, Stricker et al 2011, Wolfenson et al 2011, Yeung et al 2005).

To address the question of why there is a mechanism in place to inhibit increases in the percentage of mobile talin, but not other IAC components at adhesions, one can develop numerous potential theories. For example, this phenomenon could provide a mechanism to create plasticity in adhesions, while maintaining much of their overall stability. Evidence from multiple model systems shows that the structure of focal adhesions is very dynamic, with the components- and the importance of those components- shifting based on the needs of the cell (Geiger et al 2009). For example, in fibroblasts, when a cell senses adhesion to fibronectin fibrils, it builds a type of adhesion called a fibrillar adhesion, which is enriched in tensin, but contains low levels of paxillin and vinculin. In contrast, if that fibronectin is covalently linked to the substrate, an adhesion called a focal contact is formed, which instead

contains high levels of paxillin and vinculin (Katz et al 2000). Additionally, in *Drosophila*, dynamic morphogenetic processes in development are heavily dependent on talin interacting with integrin through IBS1, whereas interaction through IBS2 is important for stable adhesion at the MTJ (Ellis et al 2011). Maintaining some flexibility, but overall stability, during periods of low tensile force primes the complex for alteration, allowing rearrangement for important events such as repair of damage, and expansion of the MTJ during growth. The preservation of the immobile fraction increases cellular efficiency, as the production and localization of integrin and its adhesion components is energetically costly. In addition, the stability also preserves the majority of adhesion strength by keeping the important integrin-talin-actin connection intact; if the stability of that core complex is mis-regulated by increasing or decreasing recycling of integrin, the result is adhesion failure (Yuan et al 2010).

#### **4.2 Talin domains required for mechanotransduction**

The finding that talin is directly regulated by force, *in vivo*, leads to further important questions, one of which is: which of the many intra- and inter-molecular interactions that talin participates in allows mechanical force transduction? To investigate this, I used the well-established technique of structure-function analysis. Michael Fairchild mutated key domains within talin, based on research using cell culture systems, and I performed FRAP on these constructs, at MTJs, in a wildtype genetic background. The results showed that none of the tested mutations completely prevented the reduction of talin mobility in response to force. This conclusion is not as surprising as it initially seems. Talin is an extraordinarily large protein, leaving ample room for many protein-protein interactions. However, there are two interactions that are important for the conformational change that talin exhibits when force is

applied through it. One is the connection to integrin, which creates an indirect linkage to the external environment. The second is the direct connection to the actin cytoskeleton, allowing the force to be transmitted from the external environment to the supporting structure of the cell. These two types of binding domains occur at multiple places within talin. There are two characterized integrin binding sites, and at least three known actin-binding sites (Critchley & Gingras 2008), creating multiple layers of redundancy within the mechanosensitive structures of talin. This redundancy is further amplified by the fact that talin functions as a dimer within the IAC. Our lab has previously shown that if the residues of the integrin tail through which talin binds are disrupted, the mechanosensitive ability of the complex is severely impaired (Pines et al 2012). We attempted to replicate this effect in talin by using a GFP-tagged talin with mutations in both integrin-binding sites, however it did not localize to MTJs.

FRAP on talin-GFP in the context of reduced force showed that the overall percentage of mobile talin did not change significantly, however the dynamics of turnover were shifted. This result was unexpected, given our lab's previously published results on other members of the IAC (Pines et al 2012). Our lab's previous work showed that in response to decreased force, overall integrin mobility remains stable with the speed of turnover increasing, and that this effect is dependent on mechanosensing and signaling domains within integrin. This led me to test GFP-tagged talin mutants, to see if talin mobility is controlled in a similar manner. I found that only IBS2 completely re-capitulated the wildtype curve. This results shows that a strong connection to the ECM (IBS1, L334R) is required for control of talin turnover in periods of reduced force, as is talin autoinhibition, and the FERM domain.

### **4.3 Talin domains required for developmental regulation of turnover**

Previously discussed experiments were performed using temperature sensitive mutations to alter muscle contractility on demand, and at physiologically relevant levels. However, we also took advantage of the normal developmental process of muscle growth. Over the course of the five days of larval growth, the musculature increases in volume by fifteen times, and the MTJ width increases by a factor of four (Yuan et al 2010). This change in volume, and the corresponding increase in motility, mean that the adhesive junctions of the larval MTJ cope with massive increases in force over a short time.

That the overall pattern of downregulation of turnover from embryonic to larval stages is conserved is surprising, but further evidences the robustness of the complex, and the signaling network contained within it. Our lab previously examined the effect of numerous characterized integrin mutations on the pattern of turnover during development, and found many severe effects (Pines et al 2012). The discrepancy between results of FRAP using talin mutants, and previous work on integrin, could indicate that protein turnover within the IAC is primarily controlled at the level of integrin. Alternatively, as outlined above, the redundancy of each individual binding domain may compensate for any single mutation. A confounding factor is that this experiment was conducted in a genetic background with endogenous talin, meaning that two possible types of talin dimers were imaged, talin-WT with GFP-talin\*mutant, and GFP-talin\*mutant with GFP-talin\*mutant, in equal proportions, with the mixed wildtype-mutant dimer providing a mitigating effect to any effect on turnover. We attempted to reduce this by performing FRAP in a *rhea* background, which lacks endogenous

talin, however the embryos have numerous defects and die during late embryogenesis or early larval development. The final potential option is that actin binding is the important interaction for transduction of tensile force. To this end, we are currently producing a GFP-tagged talin with a mutation in the actin-binding region of the tail, and also a GFP-tagged talin with mutations in the actin-binding and dimerization domains.

Although the overall pattern of reduced mobility from embryonic to larval stages was preserved, the Headless and IBS1 mutations did show a mis-regulation of turnover between embryonic stage 16 and 17. This developmental milestone is notable for numerous reasons, one of which being that it is the transition when the musculature begins contractile activity. Disrupting IBS1, which is contained within the FERM domain, is known to severely impinge on the ability of integrins to link to the ECM (Ellis et al 2011, Tanentzapf & Brown 2006). One potential explanation for the result is that as muscles begin to contract, and forces are still relatively low, IBS1 mutants may have a slightly impaired ability to sense the growing force, but as that force continues to increase, other mechanosensors within the complex read the force input and stabilize the IAC as normal. Alternatively, other signaling methods to regulate talin stability during development may be in place. Additionally, even though IBS1 is disrupted, talin can still bind to integrin through IBS2, completing the connection to the cytoskeleton.

#### **4.4 Mechanisms for force-mediated control of adhesion stability**

Our lab previously investigated the role of force as a regulator of integrin and IAC turnover (Pines et al 2012). One of the key conclusions was that integrin endocytosis is regulated by

mechanical force. This conclusion was arrived at by fitting FRAP results to a two-parameter mathematical model. That study also examined the effect of tensile force on ILK and tensin turnover, and we attempted to model those results to determine the mechanism by which force controls IAC dynamics. However, a major obstacle prevented the generation of statistically significant conclusions about IAC turnover with the method that was in use at the time. The turnover of IAC components occurs primarily within the first 30-60 seconds after bleaching; this means that if recovery is recorded every four seconds, it produces between 8 and 15 useable data points. This lack of data means that fitting the results of FRAP to a complex model does not accurately estimate recovery kinetics. To address this, I modified the standard FRAP protocol to include three separate experiments, with different timescales and resolutions, which we then combined and fit to the model created by Dr. Raibatak Das (UC Denver). The first FRAP experiment images recovery for 75 frames at a rate of 2.5 frames/second. This captures the initial period of recovery with high fidelity, but only lasts for a short period, to reduce the effects of photobleaching, and to minimize any potential tissue damage. The second experiment images recovery for 188 frames at 1.25 frames/second, and results in an experiment half the length of the original protocol, but at five-times the resolution, resulting in only a small amount of photobleaching. Finally, the third experiment is identical to the original, imaging for 300 frames at 0.25 frames/second. This timescale allows the imaging of turnover on a long timescale with a negligible amount of photobleaching. In order to accurately fit the resulting experimental data to a mathematical model, that model has to take into account four separate processes that contribute to overall turnover. The quality of fit is significantly increased by the addition of

the two additional parameters (compared to integrin), as defined by a metric called the Akaike information criterion (Posada & Buckley 2004)

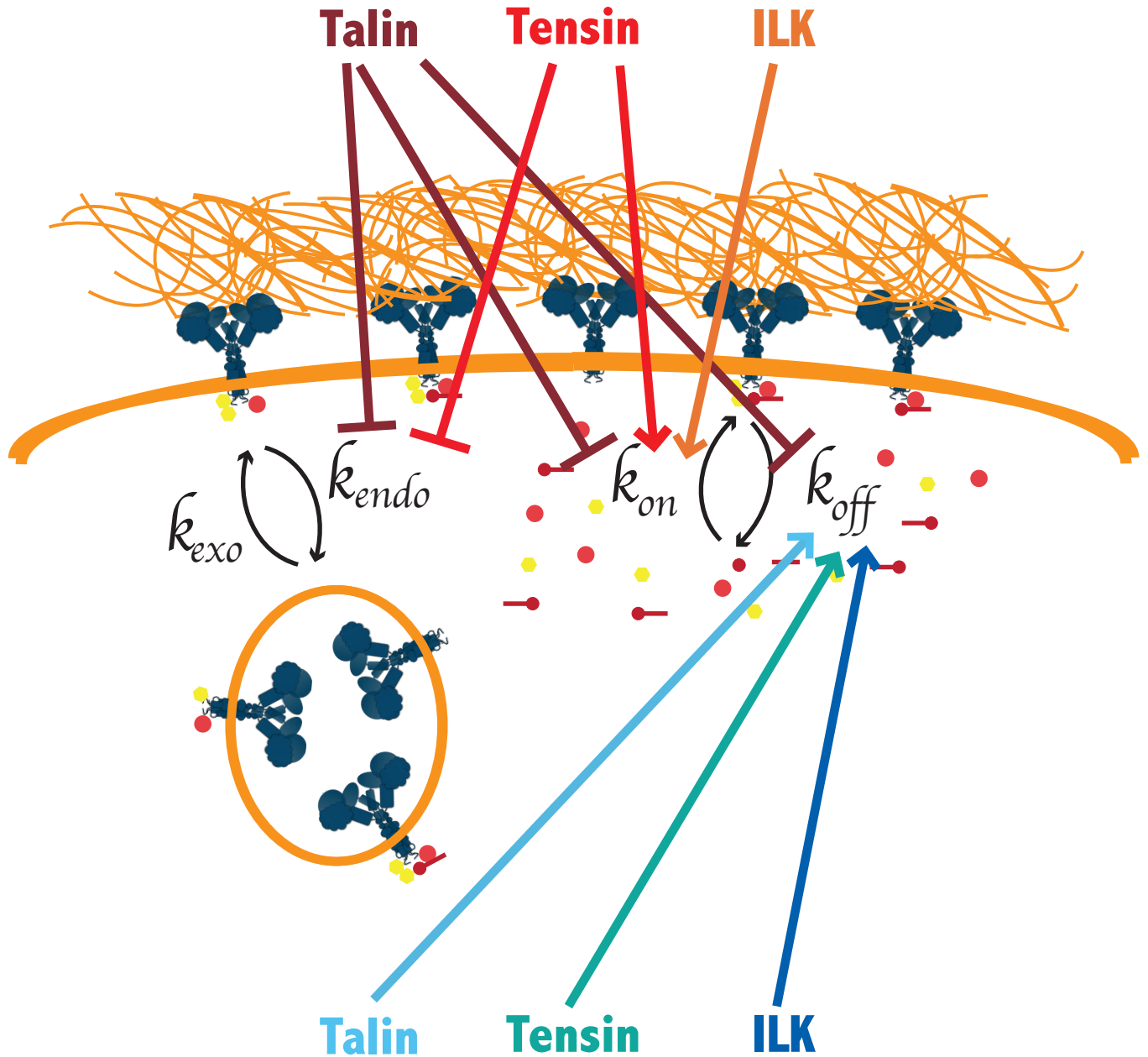
The result that fitting the FRAP data to a mathematical model accurately requires more than two parameters is not surprising. Evidence from an *in vitro* system showed that two IAC components, paxillin and vinculin, exist in four dynamic states: an immobile bound form, an adhesion-associated population undergoing exchange, and two separate populations with diffusion behavior (Wolfenson et al 2009). In our case, the populations are slightly different, as we have previously determined that diffusion does not play a major role in turnover on the timescale at which recovery occurs at the MTJ (Pines et al 2012, Yuan et al 2010). Instead, we have three populations, an immobile bound form, a population undergoing binding and unbinding (exchange) at the MTJ, and a population undergoing recycling.

Fitting the FRAP data to the model shows that each protein is regulated in a highly specific manner (Fig. 14). High force acts on each protein to increase the size of the immobile fraction, however the mechanism that causes this increase differs for each protein. With talin, the recycling rate is reduced, leaving more available talin at the membrane to incorporate into adhesions. As well, talin is more stably bound to integrin. Tensin also exhibits decreased recycling, leaving more protein at the MTJ. Finally, ILK shows increased binding affinity with adhesions, when force is increased, leading to more incorporation of ILK into the IAC.

Figure 14 – Model for the effects of force on integrin adhesion complex dynamics

# HIGH FORCE

Turnover reduced to maintain adhesion



Turnover increased to allow repair and remodeling

# low force

Reducing force has entirely different effects on those proteins. For instance, both tensin and ILK show decreased immobile populations, indicating more plasticity in the complex, but the immobile population of talin is maintained. Talin only shows an increase in unbinding that is mirrored by a similar but smaller change in the control. Tensin shows a completely different response, with a change in binding kinetics that leads to a decline in the amount of tensin bound to the adhesion complex. Lastly, in ILK, decreased force causes endocytosis, exocytosis, unbinding, and binding to increase significantly, but the magnitude of the shifts in binding versus unbinding means that the net effect is loss of ILK from the adhesion complex.

Overall, the molecular mechanism that controls protein turnover in response to force is different in each case, with talin and tensin being modulated by control of recycling and binding to the IAC, and ILK being controlled solely by shifts in its bound-state in the complex. This result contradicts previous work in cell culture showing that dynamics of IAC components are dominated by binding kinetics (Wolfenson et al 2011).

#### **4.5 Mechanisms for developmental control of adhesion stability**

Our lab has previously shown that the turnover of integrin, talin, ILK, and tensin is reduced in a stepwise manner at each developmental stage, from stage 16 embryos, to third-instar larvae (Yuan et al 2010). This change in the stability of integrin adhesions at the MTJ coincides with increases in muscle activity as development progresses through the embryonic stages, increases in muscle size and volume, and changes in motility through the larval stages. The data generated through the high-time resolution FRAP and subsequent

mathematical modeling allows us to address the question: is force the sole factor responsible for the downregulation of integrin and IAC turnover during development? The overall increase in stability concurrent to increases in force across the MTJ is consistent with the hypothesis that tensile force leads to reduced adhesion turnover. However, the result that control of turnover during development is achieved primarily through control of recycling suggests that force is not the only factor at play during embryonic and larval development. Directly increasing tensile force using the temperature sensitive *Brkd*<sup>J29</sup> mutant leads to changes in binding and recycling of tensin and talin, and in the binding, but not recycling of ILK. By contrast, as development progresses, control of recycling is the only factor in the decreased mobility of tensin and talin, and ILK mobility is reduced through control of both binding and recycling. This result is consistent with the finding that talin turnover regulation at the onset of muscle contractility requires binding to integrin through IBS1 and the talin FERM domain. If force were the only factor behind the normal downregulation, we would expect to see those same domains required for the downregulation of turnover in response to increased force triggered by the *Brkd*<sup>J29</sup> mutant, however we found that neither of those domains are required, in the genetic background used for the experiment. Additionally, talin, tensin, and ILK all have numerous interaction partners, which provides a basis for regulatory input beyond force. The talin FERM domain, for example, is known to interact with at least two proteins that regulate focal adhesion dynamics, FAK, and phosphatidylinositol (4)-phosphate 5-kinase, and there are numerous other binding partners and phosphorylation sites (Critchley & Gingras 2008, Ratnikov et al 2005, Zaidel-Bar et al 2007). ILK is well known for its role as a regulator of actin dynamics (Grashoff et al 2004), but the IPP complex is also a potent signaling hub, modulating the activity of molecules like glycogen synthase kinase 3,

and AKT/protein kinase B (Delcommenne et al 1998). As well, tensin has a Src Homology 2 domain which allows binding to tyrosine-phosphorylated proteins such as PI3 kinase, p130Cas, and FAK. This result also leaves open the possibility that slow or chronic changes in force affect the adhesion complex differently than an acute increases or decreases in force.

#### **4.6 Conclusions**

Our lab pioneered the study of adhesion dynamics in a living, multicellular organism. This thesis presents experiments that expand on that previous work on ILK and tensin, and contributes novel findings for talin. The results outlined in this work show that talin turnover is directly regulated by force in an intact complex organism, and at sites of stable adhesion between integrins and the ECM. Moreover, the results indicate that the downregulation of overall mobility from increased force is a robust process, and not easily disrupted by mutating talin domains. The stabilization of talin mobility when force is reduced is an active process, and dependent on both the physical linkage of talin to integrin, and the ability of talin to auto-inhibit. Furthermore, studies of talin, tensin, and ILK turnover with high-temporal resolution uncover the intricacies of adhesion regulation in response to changing environmental conditions; talin and tensin are regulated by a mix of both recycling and binding, and ILK is regulated through control of binding. Biophysical signaling through force is an incredibly important, but relatively poorly understood aspect of cellular signaling that can provide regulatory cues to modulate integrin-mediated adhesion. The product of this work provides novel insight relevant to how the organism properly controls turnover to maintain adhesions during development, and also to human disease, as there are a multitude

of pathologies in which cells are presented with environments with altered mechanical properties.

## Bibliography

Adams MD, Celniker SE, Holt RA, Evans CA, Gocayne JD, et al. 2000. The genome sequence of *Drosophila melanogaster*. *Science* 287: 2185-95

Aumailley M, Has C, Tunggal L, Bruckner-Tuderman L. 2006. Molecular basis of inherited skin-blistering disorders, and therapeutic implications. *Expert reviews in molecular medicine* 8: 1-21

Axelrod D, Koppel DE, Schlessinger J, Elson E, Webb WW. 1976. Mobility measurement by analysis of fluorescence photobleaching recovery kinetics. *Biophysical journal* 16: 1055-69

Balaban NQ, Schwarz US, Riveline D, Goichberg P, Tzur G, et al. 2001. Force and focal adhesion assembly: a close relationship studied using elastic micropatterned substrates. *Nat Cell Biol* 3: 466-72

Ballestrem C, Hinz B, Imhof BA, Wehrle-Haller B. 2001. Marching at the front and dragging behind: differential  $\alpha$ V $\beta$ 3-integrin turnover regulates focal adhesion behavior. *The Journal of cell biology* 155: 1319-32

Banno A, Goult BT, Lee H, Bate N, Critchley DR, Ginsberg MH. 2012. Subcellular localization of talin is regulated by inter-domain interactions. *The Journal of biological chemistry* 287: 13799-812

Barczyk M, Carracedo S, Gullberg D. 2010. Integrins. *Cell and tissue research* 339: 269-80

Bateman A, Jouet M, MacFarlane J, Du JS, Kenwrick S, Chothia C. 1996. Outline structure of the human L1 cell adhesion molecule and the sites where mutations cause neurological disorders. *The EMBO journal* 15: 6050-9

Bockholt SM, Burridge K. 1993. Cell spreading on extracellular matrix proteins induces tyrosine phosphorylation of tensin. *The Journal of biological chemistry* 268: 14565-7

Borowsky ML, Hynes RO. 1998. Layilin, a novel talin-binding transmembrane protein homologous with C-type lectins, is localized in membrane ruffles. *The Journal of cell biology* 143: 429-42

Braga J, Desterro JM, Carmo-Fonseca M. 2004. Intracellular macromolecular mobility measured by fluorescence recovery after photobleaching with confocal laser scanning microscopes. *Molecular biology of the cell* 15: 4749-60

Brancaccio M, Guazzone S, Menini N, Sibona E, Hirsch E, et al. 1999. Melusin is a new muscle-specific interactor for beta(1) integrin cytoplasmic domain. *The Journal of biological chemistry* 274: 29282-8

Bretscher MS. 1989. Endocytosis and recycling of the fibronectin receptor in CHO cells. *The EMBO journal* 8: 1341-8

- Bretscher MS. 1992. Circulating integrins: alpha 5 beta 1, alpha 6 beta 4 and Mac-1, but not alpha 3 beta 1, alpha 4 beta 1 or LFA-1. *The EMBO journal* 11: 405-10
- Broadie K, Bate M. 1993. Muscle development is independent of innervation during *Drosophila* embryogenesis. *Development* 119: 533-43
- Broussard JA, Webb DJ, Kaverina I. 2008. Asymmetric focal adhesion disassembly in motile cells. *Curr Opin Cell Biol* 20: 85-90
- Brower DL. 2003. Platelets with wings: the maturation of *Drosophila* integrin biology. *Current Opinion in Cell Biology* 15: 607-13
- Brown NH, Gregory SL, Rickoll WL, Fessler LI, Prout M, et al. 2002. Talin is essential for integrin function in *Drosophila*. *Developmental cell* 3: 569-79
- Burridge K, Connell L. 1983a. A new protein of adhesion plaques and ruffling membranes. *The Journal of cell biology* 97: 359-67
- Burridge K, Connell L. 1983b. Talin: a cytoskeletal component concentrated in adhesion plaques and other sites of actin-membrane interaction. *Cell motility* 3: 405-17
- Calderwood DA. 2004. Talin controls integrin activation. *Biochemical Society transactions* 32: 434-7

- Calderwood DA, Fujioka Y, de Pereda JM, Garcia-Alvarez B, Nakamoto T, et al. 2003. Integrin beta cytoplasmic domain interactions with phosphotyrosine-binding domains: a structural prototype for diversity in integrin signaling. *Proceedings of the National Academy of Sciences of the United States of America* 100: 2272-7
- Calderwood DA, Zent R, Grant R, Rees DJ, Hynes RO, Ginsberg MH. 1999. The Talin head domain binds to integrin beta subunit cytoplasmic tails and regulates integrin activation. *The Journal of biological chemistry* 274: 28071-4
- Calvete JJ. 2004. Structures of integrin domains and concerted conformational changes in the bidirectional signaling mechanism of alphaIIb beta3. *Exp Biol Med (Maywood)* 229: 732-44
- Campbell ID, Humphries MJ. 2011. Integrin structure, activation, and interactions. *Cold Spring Harbor perspectives in biology* 3
- Carragher NO, Levkau B, Ross R, Raines EW. 1999. Degraded collagen fragments promote rapid disassembly of smooth muscle focal adhesions that correlates with cleavage of pp125(FAK), paxillin, and talin. *The Journal of cell biology* 147: 619-30
- Caswell PT, Norman JC. 2006. Integrin trafficking and the control of cell migration. *Traffic* 7: 14-21

- Caswell PT, Vadrevu S, Norman JC. 2009. Integrins: masters and slaves of endocytic transport. *Nature reviews. Molecular cell biology* 10: 843-53
- Chen CJ, Nguyen T, Shively JE. 2010. Role of calpain-9 and PKC-delta in the apoptotic mechanism of lumen formation in CEACAM1 transfected breast epithelial cells. *Experimental cell research* 316: 638-48
- Chen NT, Lo SH. 2005. The N-terminal half of talin2 is sufficient for mouse development and survival. *Biochemical and biophysical research communications* 337: 670-6
- Choi CK, Vicente-Manzanares M, Zareno J, Whitmore LA, Mogilner A, Horwitz AR. 2008. Actin and alpha-actinin orchestrate the assembly and maturation of nascent adhesions in a myosin II motor-independent manner. *Nat Cell Biol* 10: 1039-50
- Chrzanowska-Wodnicka M, Burridge K. 1996. Rho-stimulated contractility drives the formation of stress fibers and focal adhesions. *The Journal of cell biology* 133: 1403-15
- Critchley DR, Gingras AR. 2008. Talin at a glance. *Journal of cell science* 121: 1345-7
- D'Antona G, Lanfranconi F, Pellegrino MA, Brocca L, Adami R, et al. 2006. Skeletal muscle hypertrophy and structure and function of skeletal muscle fibres in male body builders. *The Journal of physiology* 570: 611-27

Davis S, Lu ML, Lo SH, Lin S, Butler JA, et al. 1991. Presence of an SH2 domain in the actin-binding protein tensin. *Science* 252: 712-5

del Rio A, Perez-Jimenez R, Liu R, Roca-Cusachs P, Fernandez JM, Sheetz MP. 2009. Stretching single talin rod molecules activates vinculin binding. *Science* 323: 638-41

Delcommenne M, Tan C, Gray V, Rue L, Woodgett J, Dedhar S. 1998. Phosphoinositide-3-OH kinase-dependent regulation of glycogen synthase kinase 3 and protein kinase B/AKT by the integrin-linked kinase. *Proceedings of the National Academy of Sciences of the United States of America* 95: 11211-6

Dourdin N, Bhatt AK, Dutt P, Greer PA, Arthur JS, et al. 2001. Reduced cell migration and disruption of the actin cytoskeleton in calpain-deficient embryonic fibroblasts. *The Journal of biological chemistry* 276: 48382-8

Edgerton VR, Zhou MY, Ohira Y, Klitgaard H, Jiang B, et al. 1995. Human fiber size and enzymatic properties after 5 and 11 days of spaceflight. *J Appl Physiol* 78: 1733-39

Edidin M, Zagyansky Y, Lardner TJ. 1976. Measurement of membrane protein lateral diffusion in single cells. *Science* 191: 466-8

Ellis SJ, Pines M, Fairchild MJ, Tanentzapf G. 2011. In vivo functional analysis reveals specific roles for the integrin-binding sites of talin. *Journal of cell science* 124: 1844-

- Ezratty EJ, Bertaux C, Marcantonio EE, Gundersen GG. 2009. Clathrin mediates integrin endocytosis for focal adhesion disassembly in migrating cells. *The Journal of cell biology* 187: 733-47
- Farge E. 2003. Mechanical Induction of Twist in the Drosophila Foregut/Stomodaeal Primordium. *Current Biology* 13: 1365-77
- Fluck M, Hoppeler H. 2003. Molecular basis of skeletal muscle plasticity--from gene to form and function. *Reviews of physiology, biochemistry and pharmacology* 146: 159-216
- Franco SJ, Huttenlocher A. 2005. Regulating cell migration: calpains make the cut. *Journal of cell science* 118: 3829-38
- Franco SJ, Rodgers MA, Perrin BJ, Han J, Bennin DA, et al. 2004. Calpain-mediated proteolysis of talin regulates adhesion dynamics. *Nat Cell Biol* 6: 977-83
- Friedland JC, Lee MH, Boettiger D. 2009. Mechanically activated integrin switch controls alpha5beta1 function. *Science* 323: 642-4
- Galbraith CG, Yamada KM, Sheetz MP. 2002. The relationship between force and focal complex development. *The Journal of cell biology* 159: 695-705
- Garcia-Alvarez B, de Pereda JM, Calderwood DA, Ulmer TS, Critchley D, et al. 2003. Structural determinants of integrin recognition by talin. *Molecular cell* 11: 49-58

Geiger B, Spatz JP, Bershadsky AD. 2009. Environmental sensing through focal adhesions. *Nature reviews. Molecular cell biology* 10: 21-33

Geiger B, Yamada KM. 2011. Molecular architecture and function of matrix adhesions. *Cold Spring Harbor perspectives in biology* 3

Ginsberg MH, Partridge A, Shattil SJ. 2005. Integrin regulation. *Curr Opin Cell Biol* 17: 509-16

Glading A, Lauffenburger DA, Wells A. 2002. Cutting to the chase: calpain proteases in cell motility. *Trends in cell biology* 12: 46-54

Goksoy E, Ma YQ, Wang X, Kong X, Perera D, et al. 2008. Structural basis for the autoinhibition of talin in regulating integrin activation. *Molecular cell* 31: 124-33

Golden A, Nemeth SP, Brugge JS. 1986. Blood platelets express high levels of the pp60c-src-specific tyrosine kinase activity. *Proceedings of the National Academy of Sciences of the United States of America* 83: 852-6

Goult BT, Bate N, Anthis NJ, Wegener KL, Gingras AR, et al. 2009. The structure of an interdomain complex that regulates talin activity. *The Journal of biological chemistry* 284: 15097-106

- Grashoff C, Hoffman BD, Brenner MD, Zhou R, Parsons M, et al. 2010. Measuring mechanical tension across vinculin reveals regulation of focal adhesion dynamics. *Nature* 466: 263-6
- Grashoff C, Thievensen I, Lorenz K, Ussar S, Fassler R. 2004. Integrin-linked kinase: integrin's mysterious partner. *Curr Opin Cell Biol* 16: 565-71
- Hahn C, Schwartz MA. 2009. Mechanotransduction in vascular physiology and atherogenesis. *Nature reviews. Molecular cell biology* 10: 53-62
- Hannigan G, Troussard AA, Dedhar S. 2005. Integrin-linked kinase: a cancer therapeutic target unique among its ILK. *Nature reviews. Cancer* 5: 51-63
- Hannigan GE, Leung-Hagesteijn C, Fitz-Gibbon L, Coppolino MG, Radeva G, et al. 1996. Regulation of cell adhesion and anchorage-dependent growth by a new beta 1-integrin-linked protein kinase. *Nature* 379: 91-6
- Heggeness MH, Wang K, Singer SJ. 1977. Intracellular distributions of mechanochemical proteins in cultured fibroblasts. *Proceedings of the National Academy of Sciences of the United States of America* 74: 3883-7
- Helsten TL, Bunch TA, Kato H, Yamanouchi J, Choi SH, et al. 2008. Differences in regulation of Drosophila and vertebrate integrin affinity by talin. *Molecular biology of the cell* 19: 3589-98

- Huang MM, Bolen JB, Barnwell JW, Shattil SJ, Brugge JS. 1991. Membrane glycoprotein IV (CD36) is physically associated with the Fyn, Lyn, and Yes protein-tyrosine kinases in human platelets. *Proceedings of the National Academy of Sciences of the United States of America* 88: 7844-8
- Hudson AM, Petrella LN, Tanaka AJ, Cooley L. 2008. Mononuclear muscle cells in *Drosophila* ovaries revealed by GFP protein traps. *Developmental biology* 314: 329-40
- Humphries JD, Byron A, Humphries MJ. 2006. Integrin ligands at a glance. *Journal of cell science* 119: 3901-3
- Huttenlocher A, Palecek SP, Lu Q, Zhang W, Mellgren RL, et al. 1997. Regulation of cell migration by the calcium-dependent protease calpain. *The Journal of biological chemistry* 272: 32719-22
- Hynes RO. 2002. A reevaluation of integrins as regulators of angiogenesis. *Nature medicine* 8: 918-21
- Jiang G, Giannone G, Critchley DR, Fukumoto E, Sheetz MP. 2003. Two-piconewton slip bond between fibronectin and the cytoskeleton depends on talin. *Nature* 424: 334-7

Jin M, Andricioaei I, Springer TA. 2004. Conversion between three conformational states of integrin I domains with a C-terminal pull spring studied with molecular dynamics. *Structure* 12: 2137-47

Katsumi A, Naoe T, Matsushita T, Kaibuchi K, Schwartz MA. 2005. Integrin activation and matrix binding mediate cellular responses to mechanical stretch. *The Journal of biological chemistry* 280: 16546-9

Katz BZ, Zamir E, Bershadsky A, Kam Z, Yamada KM, Geiger B. 2000. Physical state of the extracellular matrix regulates the structure and molecular composition of cell-matrix adhesions. *Molecular biology of the cell* 11: 1047-60

Kloeker S, Major MB, Calderwood DA, Ginsberg MH, Jones DA, Beckerle MC. 2004. The Kindler syndrome protein is regulated by transforming growth factor-beta and involved in integrin-mediated adhesion. *The Journal of biological chemistry* 279: 6824-33

Knoll R, Postel R, Wang J, Kratzner R, Hennecke G, et al. 2007. Laminin-alpha4 and integrin-linked kinase mutations cause human cardiomyopathy via simultaneous defects in cardiomyocytes and endothelial cells. *Circulation* 116: 515-25

Krishna SM, Dear AE, Norman PE, Golledge J. 2010. Genetic and epigenetic mechanisms and their possible role in abdominal aortic aneurysm. *Atherosclerosis* 212: 16-29

- Kusumi A, Sako Y, Yamamoto M. 1993. Confined lateral diffusion of membrane receptors as studied by single particle tracking (nanovid microscopy). Effects of calcium-induced differentiation in cultured epithelial cells. *Biophysical journal* 65: 2021-40
- Le Clainche C, Dwivedi SP, Didry D, Carlier MF. 2010. Vinculin is a dually regulated actin filament barbed end-capping and side-binding protein. *The Journal of biological chemistry* 285: 23420-32
- Leblanc AD, Schneider VS, Evans HJ, Engelbretson DA, Krebs JM. 1990. Bone mineral loss and recovery after 17 weeks of bed rest. *Journal of Bone and Mineral Research* 5: 843-50
- Legate KR, Montanez E, Kudlacek O, Fassler R. 2006. ILK, PINCH and parvin: the tIPP of integrin signalling. *Nature reviews. Molecular cell biology* 7: 20-31
- Lionetti V, Recchia FA, Marco Ranieri V. 2005. Overview of ventilator-induced lung injury mechanisms. *Current Opinion in Critical Care* 11: 82-86
- Lo SH. 2004. Tensin. *The international journal of biochemistry & cell biology* 36: 31-4
- Lo SH, Janmey PA, Hartwig JH, Chen LB. 1994. Interactions of tensin with actin and identification of its three distinct actin-binding domains. *The Journal of cell biology* 125: 1067-75

- Loer B, Bauer R, Bornheim R, Grell J, Kremmer E, et al. 2008. The NHL-domain protein Wech is crucial for the integrin-cytoskeleton link. *Nat Cell Biol* 10: 422-8
- Lucitti JL, Jones EA, Huang C, Chen J, Fraser SE, Dickinson ME. 2007. Vascular remodeling of the mouse yolk sac requires hemodynamic force. *Development* 134: 3317-26
- Mackinnon AC, Qadota H, Norman KR, Moerman DG, Williams BD. 2002. C. elegans PAT-4/ILK functions as an adaptor protein within integrin adhesion complexes. *Current biology : CB* 12: 787-97
- Miyamoto S, Akiyama SK, Yamada KM. 1995a. Synergistic roles for receptor occupancy and aggregation in integrin transmembrane function. *Science* 267: 883-5
- Miyamoto S, Teramoto H, Coso OA, Gutkind JS, Burbelo PD, et al. 1995b. Integrin function: molecular hierarchies of cytoskeletal and signaling molecules. *The Journal of cell biology* 131: 791-805
- Monkley SJ, Zhou XH, Kinston SJ, Giblett SM, Hemmings L, et al. 2000. Disruption of the talin gene arrests mouse development at the gastrulation stage. *Developmental dynamics : an official publication of the American Association of Anatomists* 219: 560-74

- Montana ES, Littleton JT. 2004. Characterization of a hypercontraction-induced myopathy in *Drosophila* caused by mutations in Mhc. *The Journal of cell biology* 164: 1045-54
- Mosesson Y, Mills GB, Yarden Y. 2008. Derailed endocytosis: an emerging feature of cancer. *Nature reviews. Cancer* 8: 835-50
- Nieswandt B, Moser M, Pleines I, Varga-Szabo D, Monkley S, et al. 2007. Loss of talin1 in platelets abrogates integrin activation, platelet aggregation, and thrombus formation in vitro and in vivo. *The Journal of experimental medicine* 204: 3113-8
- Nikolopoulos SN, Turner CE. 2000. Actopaxin, a new focal adhesion protein that binds paxillin LD motifs and actin and regulates cell adhesion. *The Journal of cell biology* 151: 1435-48
- Norgett EE, Hatsell SJ, Carvajal-Huerta L, Cabezas JC, Common J, et al. 2000. Recessive mutation in desmoplakin disrupts desmoplakin-intermediate filament interactions and causes dilated cardiomyopathy, woolly hair and keratoderma. *Human molecular genetics* 9: 2761-6
- O'Dowd DK, Germeraad SE, Aldrich RW. 1989. Alterations in the expression and gating of *Drosophila* sodium channels by mutations in the para gene. *Neuron* 2: 1301-11

- Pankov R, Cukierman E, Katz BZ, Matsumoto K, Lin DC, et al. 2000. Integrin dynamics and matrix assembly: tensin-dependent translocation of alpha(5)beta(1) integrins promotes early fibronectin fibrillogenesis. *The Journal of cell biology* 148: 1075-90
- Parsons JT, Horwitz AR, Schwartz MA. 2010. Cell adhesion: integrating cytoskeletal dynamics and cellular tension. *Nature reviews. Molecular cell biology* 11: 633-43
- Pasquet JM, Noury M, Nurden AT. 2002. Evidence that the platelet integrin alphaIIb beta3 is regulated by the integrin-linked kinase, ILK, in a PI3-kinase dependent pathway. *Thrombosis and haemostasis* 88: 115-22
- Paszek MJ, Zahir N, Johnson KR, Lakins JN, Rozenberg GI, et al. 2005. Tensional homeostasis and the malignant phenotype. *Cancer cell* 8: 241-54
- Pelham RJ, Jr., Wang Y. 1997. Cell locomotion and focal adhesions are regulated by substrate flexibility. *Proceedings of the National Academy of Sciences of the United States of America* 94: 13661-5
- Pellinen T, Arjonen A, Vuoriluoto K, Kallio K, Fransén JA, Ivaska J. 2006. Small GTPase Rab21 regulates cell adhesion and controls endosomal traffic of beta1-integrins. *The Journal of cell biology* 173: 767-80
- Pellinen T, Ivaska J. 2006. Integrin traffic. *Journal of cell science* 119: 3723-31

- Perkins AD, Ellis SJ, Asghari P, Shamsian A, Moore ED, Tanentzapf G. 2010. Integrin-mediated adhesion maintains sarcomeric integrity. *Developmental biology* 338: 15-27
- Pestina TI, Stenberg PE, Druker BJ, Steward SA, Hutson NK, et al. 1997. Identification of the Src family kinases, Lck and Fgr in platelets. Their tyrosine phosphorylation status and subcellular distribution compared with other Src family members. *Arteriosclerosis, thrombosis, and vascular biology* 17: 3278-85
- Peters R, Peters J, Tews KH, Bahr W. 1974. A microfluorimetric study of translational diffusion in erythrocyte membranes. *Biochimica et biophysica acta* 367: 282-94
- Petrich BG, Marchese P, Ruggeri ZM, Spiess S, Weichert RA, et al. 2007. Talin is required for integrin-mediated platelet function in hemostasis and thrombosis. *The Journal of experimental medicine* 204: 3103-11
- Pines M, Das R, Ellis SJ, Morin A, Czerniecki S, et al. 2012. Mechanical force regulates integrin turnover in *Drosophila* in vivo. *Nat Cell Biol* 14: 935-43
- Pittendrigh B, Reenan R, ffrench-Constant RH, Ganetzky B. 1997. Point mutations in the *Drosophila* sodium channel gene para associated with resistance to DDT and pyrethroid insecticides. *Molecular & general genetics : MGG* 256: 602-10

- Posada D, Buckley TR. 2004. Model selection and model averaging in phylogenetics: advantages of akaike information criterion and bayesian approaches over likelihood ratio tests. *Systematic biology* 53: 793-808
- Press WH. 2007. *Numerical recipes : the art of scientific computing*. Cambridge, UK ; New York: Cambridge University Press. xxi, 1235 p. pp.
- Price MG. 1987. Skelemins: cytoskeletal proteins located at the periphery of M-discs in mammalian striated muscle. *The Journal of cell biology* 104: 1325-36
- Puklin-Faucher E, Gao M, Schulten K, Vogel V. 2006. How the headpiece hinge angle is opened: New insights into the dynamics of integrin activation. *The Journal of cell biology* 175: 349-60
- Pulkkinen L, Christiano AM, Airenne T, Haakana H, Tryggvason K, Uitto J. 1994. Mutations in the gamma 2 chain gene (LAMC2) of kalinin/laminin 5 in the junctional forms of epidermolysis bullosa. *Nature genetics* 6: 293-7
- Ratnikov B, Ptak C, Han J, Shabanowitz J, Hunt DF, Ginsberg MH. 2005. Talin phosphorylation sites mapped by mass spectrometry. *Journal of cell science* 118: 4921-3
- Reits EA, Neefjes JJ. 2001. From fixed to FRAP: measuring protein mobility and activity in living cells. *Nat Cell Biol* 3: E145-7

- Rendu F, Lebret M, Danielian S, Fagard R, Levy-Toledano S, Fischer S. 1989. High pp60c-src level in human platelet dense bodies. *Blood* 73: 1545-51
- Robling AG, Castillo AB, Turner CH. 2006. Biomechanical and molecular regulation of bone remodeling. *Annual review of biomedical engineering* 8: 455-98
- Sakai T, Li S, Docheva D, Grashoff C, Sakai K, et al. 2003. Integrin-linked kinase (ILK) is required for polarizing the epiblast, cell adhesion, and controlling actin accumulation. *Genes & development* 17: 926-40
- Schaller MD, Borgman CA, Cobb BS, Vines RR, Reynolds AB, Parsons JT. 1992. pp125FAK a structurally distinctive protein-tyrosine kinase associated with focal adhesions. *Proceedings of the National Academy of Sciences of the United States of America* 89: 5192-6
- Schaper W. 2009. Collateral circulation: past and present. *Basic Res Cardiol* 104: 5-21
- Schiffrin EL. 1992. Reactivity of small blood vessels in hypertension: relation with structural changes. State of the art lecture. *Hypertension* 19: II1-9
- Schwartz MA. 2010. Integrins and extracellular matrix in mechanotransduction. *Cold Spring Harbor perspectives in biology* 2: a005066

- Somogyi K, Rorth P. 2004. Evidence for tension-based regulation of Drosophila MAL and SRF during invasive cell migration. *Developmental cell* 7: 85-93
- Sorkin A, von Zastrow M. 2009. Endocytosis and signalling: intertwining molecular networks. *Nature reviews. Molecular cell biology* 10: 609-22
- Stark KA, Yee GH, Roote CE, Williams EL, Zusman S, Hynes RO. 1997. A novel alpha integrin subunit associates with betaPS and functions in tissue morphogenesis and movement during Drosophila development. *Development* 124: 4583-94
- Stricker J, Aratyn-Schaus Y, Oakes PW, Gardel ML. 2011. Spatiotemporal constraints on the force-dependent growth of focal adhesions. *Biophysical journal* 100: 2883-93
- Suzuki DT, Grigliatti T, Williamson R. 1971. Temperature-sensitive mutations in Drosophila melanogaster. VII. A mutation (para-ts) causing reversible adult paralysis. *Proceedings of the National Academy of Sciences of the United States of America* 68: 890-3
- Tadokoro S, Shattil SJ, Eto K, Tai V, Liddington RC, et al. 2003. Talin binding to integrin beta tails: a final common step in integrin activation. *Science* 302: 103-6
- Tanentzapf G, Brown NH. 2006. An interaction between integrin and the talin FERM domain mediates integrin activation but not linkage to the cytoskeleton. *Nat Cell Biol* 8: 601-6

- Thodeti CK, Matthews B, Ravi A, Mammoto A, Ghosh K, et al. 2009. TRPV4 channels mediate cyclic strain-induced endothelial cell reorientation through integrin-to-integrin signaling. *Circulation research* 104: 1123-30
- Torgler CN, Narasimha M, Knox AL, Zervas CG, Vernon MC, Brown NH. 2004. Tensin stabilizes integrin adhesive contacts in *Drosophila*. *Developmental cell* 6: 357-69
- Tu Y, Li F, Goicoechea S, Wu C. 1999. The LIM-only protein PINCH directly interacts with integrin-linked kinase and is recruited to integrin-rich sites in spreading cells. *Molecular and cellular biology* 19: 2425-34
- Tucker KL, Sage T, Stevens JM, Jordan PA, Jones S, et al. 2008. A dual role for integrin-linked kinase in platelets: regulating integrin function and alpha-granule secretion. *Blood* 112: 4523-31
- Turner CE, Glenney JR, Jr., Burridge K. 1990. Paxillin: a new vinculin-binding protein present in focal adhesions. *The Journal of cell biology* 111: 1059-68
- Voeller HJ, Truica CI, Gelmann EP. 1998. Beta-catenin mutations in human prostate cancer. *Cancer research* 58: 2520-3
- Volk T, VijayRaghavan K. 1994. A central role for epidermal segment border cells in the induction of muscle patterning in the *Drosophila* embryo. *Development* 120: 59-70

- Wasserman L. 2004. *All of statistics : a concise course in statistical inference*. New York: Springer. xix, 442 p. pp.
- Webb DJ, Parsons JT, Horwitz AF. 2002. Adhesion assembly, disassembly and turnover in migrating cells -- over and over and over again. *Nat Cell Biol* 4: E97-100
- Wegener KL, Campbell ID. 2008. Transmembrane and cytoplasmic domains in integrin activation and protein-protein interactions (review). *Molecular membrane biology* 25: 376-87
- Wegener KL, Partridge AW, Han J, Pickford AR, Liddington RC, et al. 2007. Structural basis of integrin activation by talin. *Cell* 128: 171-82
- Wehland J, Weber K, Gawlitta W, Stockem W. 1979. Effects of the actin-binding protein DNAase I on cytoplasmic streaming and ultrastructure of *Amoeba proteus*. An attempt to explain amoeboid movement. *Cell and tissue research* 199: 353-72
- Wehrle-Haller B. 2007. Analysis of integrin dynamics by fluorescence recovery after photobleaching. *Methods Mol Biol* 370: 173-202
- Wilcox M, Brower DL, Smith RJ. 1981. A position-specific cell surface antigen in the drosophila wing imaginal disc. *Cell* 25: 159-64

- Wilkins JA, Risinger MA, Lin S. 1986. Studies on proteins that co-purify with smooth muscle vinculin: identification of immunologically related species in focal adhesions of nonmuscle and Z-lines of muscle cells. *The Journal of cell biology* 103: 1483-94
- Wolfenson H, Bershadsky A, Henis YI, Geiger B. 2011. Actomyosin-generated tension controls the molecular kinetics of focal adhesions. *Journal of cell science* 124: 1425-32
- Wolfenson H, Lubelski A, Regev T, Klafter J, Henis YI, Geiger B. 2009. A role for the juxtamembrane cytoplasm in the molecular dynamics of focal adhesions. *PloS one* 4: e4304
- Wright TR. 1960. The phenogenetics of the embryonic mutant, lethal myospheroid, in *Drosophila melanogaster*. *The Journal of experimental zoology* 143: 77-99
- Yeung T, Georges PC, Flanagan LA, Marg B, Ortiz M, et al. 2005. Effects of substrate stiffness on cell morphology, cytoskeletal structure, and adhesion. *Cell motility and the cytoskeleton* 60: 24-34
- Yuan L, Fairchild MJ, Perkins AD, Tanentzapf G. 2010. Analysis of integrin turnover in fly myotendinous junctions. *Journal of cell science* 123: 939-46
- Zaidel-Bar R, Geiger B. 2010. The switchable integrin adhesome. *Journal of cell science* 123: 1385-8

Zaidel-Bar R, Itzkovitz S, Ma'ayan A, Iyengar R, Geiger B. 2007. Functional atlas of the integrin adhesome. *Nat Cell Biol* 9: 858-67

Zamir E, Katz BZ, Aota S, Yamada KM, Geiger B, Kam Z. 1999. Molecular diversity of cell-matrix adhesions. *Journal of cell science* 112 ( Pt 11): 1655-69

Zervas CG, Gregory SL, Brown NH. 2001. Drosophila integrin-linked kinase is required at sites of integrin adhesion to link the cytoskeleton to the plasma membrane. *The Journal of cell biology* 152: 1007-18

Zhang X, Jiang G, Cai Y, Monkley SJ, Critchley DR, Sheetz MP. 2008. Talin depletion reveals independence of initial cell spreading from integrin activation and traction. *Nat Cell Biol* 10: 1062-8

Zhu J, Luo BH, Xiao T, Zhang C, Nishida N, Springer TA. 2008. Structure of a complete integrin ectodomain in a physiologic resting state and activation and deactivation by applied forces. *Molecular cell* 32: 849-61